Marine Geology 345 (2013) 266–280

Contents lists available at ScienceDirect

Marine Geology

journal homepage: www.elsevier.com/locate/margeo

Factors controlling floc settling velocity along a longitudinal estuarine transect

A.J. Manning [a,b,c,*], D.H. Schoellhamer [d,e]

[a] HR Wallingford, Howbery Park, Wallingford, Oxfordshire OX10 8BA, UK
[b] School of Marine Science & Engineering, University of Plymouth, Drake Circus, Plymouth, Devon PL4 8AA, UK
[c] Department of Geography, Environment and Earth Sciences, University of Hull, Hull HU6 7RX, UK
[d] U.S. Geological Survey, Placer Hall, 6000 J Street, Sacramento, CA 95819, USA
[e] Department of Civil & Environmental Engineering, University of California, Davis, USA

ARTICLE INFO

Article history:
Received 4 July 2012
Received in revised form 23 June 2013
Accepted 24 June 2013
Available online 5 July 2013

Keywords:
San Francisco Bay
flocculation
settling velocity
suspended sediment concentration
cohesive sediment
mixed sediment
macrofloc
INSSEV-LF
mass settling flux

ABSTRACT

A 147 km longitudinal transect of flocculated cohesive sediment properties in San Francisco Bay (SFB) was conducted on June 17th, 2008. Our aim was to determine the factors that control floc settling velocity along the longitudinal axis of the estuary. The INSSEV-LF video system was used to measure floc diameters and settling velocities at 30 stations at a distance of 0.7 m above the estuary bed. Floc sizes (D) ranged from 22 μm to 639 μm and settling velocities (Ws) ranged between 0.04 $mm \cdot s^{-1}$ and 15.8 $mm \cdot s^{-1}$ during the longitudinal transect. Nearbed turbulent shear stresses throughout the transect duration were within the 0.2–0.5 Pa range which typically stimulates flocculation growth. The individual D–Ws–floc density plots suggest the suspended sediments encountered throughout SFB were composed of both muddy cohesive sediment and mixed sediments flocs. Mass-weighted population mean settling velocity (Ws_{mass}) ranged from 0.5 $mm \cdot s^{-1}$ to 10 $mm \cdot s^{-1}$. The macrofloc and microfloc (demarcation at 160 μm) sub-populations demonstrated parameterised settling velocities which spanned nearly double the range of the sample mean settling velocities (Ws_{mean}). The macroflocs tended to dominate the suspended mass (up to 77% of the ambient suspended solid concentration; SSC) from San Pablo Bay to Carquinez Strait (the vicinity of the turbidity maximum zone). Microfloc mass was particularly significant (typically 60–100% of the SSC) in the northern section of South Bay and most of Central Bay. The transect took eleven hours to complete and was not fully synoptic. During slack tide, larger and faster settling flocs deposited, accounting for most of the longitudinal variability. The best single predictor of settling velocity was water velocity 39 min prior to sampling, not suspended-sediment concentration or salinity. Resuspension and settling lags are likely responsible for the lagged response of settling velocity to water velocity. The distribution of individual floc diameters and settling velocities indicates that floc density for a given floc diameter varies greatly. A small portion (a few percent) of suspended sediment mass in SFB is sand-sized and inclusion of sand in flocs appears likely. Fractal theory for cohesive sediment assumes that there is a single primary particle size that flocculates, which is not the case for these types of mixed sediment flocs. The wide variability in the physical, biological and chemical processes which contribute to flocculation within SFB means that spatial floc data is required in order to accurately represent the diverse floc dynamics present in the Bay system. The importance in determining accurate estimates of floc density has been highlighted by the SFB data, as these provide the basis for realistic distributions of floc dry mass and the mass settling flux across a floc population. However, although video floc sampling devices can produce the various floc property trends observed in SFB, good survey practice is still paramount. One can see that if the sampling coverage (i.e. data collection frequency) is poor, this could lead to potential mis-interpretations of the data and only limited conclusions may be drawn from such a restricted survey. For example, a limited survey (i.e. only 3 stations, compared to the 10 stations in the full survey) in South Bay produces an under-estimate in both the macrofloc SSC_{macro} distribution by a factor of four and the Ws_{macro} by a factor of two. To develop sediment transport numerical models for SFB, high quality floc size and settling data are needed to understand and simulate the depositional qualities of both suspended cohesive sediment and mixed sediments in San Francisco Bay. This study has shown that the most pragmatic solution is a physically-based approach, whereby the detailed flocs D vs. Ws spectra are parameterised in terms of their macrofloc and microfloc properties. This aids in model calibration, whilst retaining more of

* Corresponding author at: HR Wallingford, Howbery Park, Wallingford, Oxfordshire OX10 8BA, UK. Fax: +44 1491 832233.
E-mail addresses: andymanning@yahoo.com (A.J. Manning), dschoell@usgs.gov (D.H. Schoellhamer).

0025-3227/$ – see front matter
http://dx.doi.org/10.1016/j.margeo.2013.06.018

the dynamical aspects of the floc populations. All forms of flocculation are dynamically active processes, therefore it is important to also include both SSC and turbulence functions together with the floc data.

1. Introduction

Much of the sediment within San Francisco Bay (SFB) is cohesive and can therefore act as transport mechanism for pollutants which adsorb to clay minerals. Furthermore, muddy sediment can flocculate when resuspended; this significantly alters their transport characteristics, which poses a serious complication to the modelling of sediment pathways. As flocs grow in size (D) their effective density ρ_e. (i.e. bulk density less the water density) generally decreases (Gibbs, 1985; Droppo et al., 2000). However due to a Stokes' law relationship, their settling velocity (Ws) tends to quicken with increasing floc diameter (Dyer and Manning, 1999). Thus, there is a three-way interrelationship between D:Ws:ρ_e.

Several factors can affect flocculation and in particular the settling velocity of flocs. The degree of flocculation, often referred to as the *stability* (van Leussen, 1994), is highly dependent upon a number of parameters, including: mineralogy (Winterwerp and van Kesteren, 2004); electrolytic levels which tend to be altered through salinity in an estuary (Krone, 1963), which can in turn affect the zeta-potential of clay particles (Chassagne et al., 2009); suspended sediment concentration (SSC; Burban et al., 1989); organic content (Kranck, 1984), and turbulent mixing (e.g. Winterwerp, 1998; Manning, 2004a). A conceptual model which attempts to explain the linkage between floc structure and floc behaviour in an aquatic environment is provided by Droppo (2001).

Flocculation occurs more rapidly when salinity exceeds 1 to 2 in laboratory experiments (Krone, 1962). Edzwald and O'Melia (1975) conducted experiments with kaolinite, and found that the efficiency of electrostatic flocculation was only 10% or less; primarily due to the weakness of the electrostatic bonds. However Alldredge and Silver (1988) found that for particles coated with natural polymers the efficiency could reach 100%. The relevance of salt flocculation in estuaries has increasingly been questioned because of the potential greater influence of sticky organic material present in natural mud, for example those derived from biota which can secrete sticky extracellular polymeric substances (EPSs; e.g. Tolhurst et al., 2002).

Experiments by Kranck (1984) have shown that the flocculation of mineral particles which contained some organic matter greatly enhanced the settling velocity of the aggregates. Flocculation potential and the resultant settling velocity can also increase as SSC increases, up to the point of hindered settling (Mehta, 1989). Turbulence creates inter-particle collisions and stimulates flocculation (McAnally and Mehta, 2001); however too much turbulence though can break flocs apart. McCave (1984) found that turbulence determines the maximum floc size in tidally dominated estuaries. Fettweis et al. (2006) showed floc size and the Kolmogorov microscale varies similarly with the root mean square of the gradient in the turbulent velocity fluctuations.

Cohesive sediment in an estuary initially flocculates into small microflocs. During more floc-conducive conditions, microflocs combine to form larger macroflocs (Eisma, 1986; Krone, 1986). In terms of flocculation kinetics (Overbeek, 1952), the highly porous and low density macroflocs tend to control the fate of purely muddy sediment in an estuary (Mikeš and Manning, 2010), because the smaller microflocs generally settle at less than 1 $mm \cdot s^{-1}$, whereas macroflocs settle in the 1–15 $mm \cdot s^{-1}$ range, enabling them to deposit to the bed (Pouët, 1997). However, when mixed sediment flocculation occurs, the microflocs can potentially demonstrate settling velocities comparable to those of the macroflocs (Manning et al., 2013).

Much of the pioneering work in this field was conducted in the laboratory (e.g. Krone, 1963) and predated optical methods for directly observing and measuring floc diameter and settling velocity. Most flocculation surveys tend to focus on a limited number of point measurements in an estuary, as these observations tend to be for advection–diffusion numerical sediment transport model calibration. Observation along estuarine longitudinal axes of floc properties with optical methods measuring the floc properties and the factors that potentially control floc settling velocity are rare, due to: i) a lack of proven optical floc sampling devices which can simultaneously measure D and Ws; ii) the complex logistics of measuring floc properties at multiple locations; iii) the cost involved in organising such a large spatial field survey campaign; iv) and a general lack of available expertise in processing and calibrating high volumes of digital floc video images. Most of the previous surveys focused solely on floc size, or indirect floc observations through gravimetric analysis of water samples collected with field settling tube (e.g. Owen, 1976).

The aim of this paper is to determine the factors that affect floc settling velocity along a longitudinal transect in an estuary. We collected and analysed data on flocs and on potential controlling factors along a 147 km transect the length of San Francisco Bay, USA, on June 17th, 2008. A selection of floc data will be presented and discussed. As the data was collected in conjunction with spatial water quality monitoring of SFB, it was anticipated that the floc information will provide some insight into the mobility of the suspended sediment within SFB and how this may affect water quality issues.

2. Study location

San Francisco Bay (SFB) is a predominantly shallow, drowned river valley type estuary, with an ebb dominant tidal regime. The estuary receives inflow from both the Sacramento and San Joaquin rivers, which originate from the Sierra Nevada Mountains. These drain the Central Valley watershed which comprises 154,000 km^2 or approximately 37% of the area of the State of California (McKee et al., 2006), which eventually drains in the Pacific Ocean. All of the smaller local watersheds adjacent to the Bay supply about 10% of the freshwater but the same quantity of sediment as the Central Valley (Conomos and Peterson, 1977; Schoellhamer et al., 2005). Most of the supply of water and sediment is delivered during the wet season, approximately November to March. Wright and Schoellhamer (2005) analysed hydrographs and sediment loads from the Central Valley from 1998 to 2002 and found that wet periods constituted only 31% of the total time, but the majority of sediment was delivered during these wet periods (82%).

Geographically, San Francisco Bay comprises a number of interconnected smaller bays. Northern San Francisco Bay is a classic estuary with a longitudinal salinity gradient whilst during the dry season South San Francisco Bay more closely resembles a lagoon with nearly homogeneous salinity. San Francisco Bay drains to the Pacific Ocean. The Sacramento and San Joaquin rivers initially flow into Suisun Bay, and this is connected to Carquinez Strait to the west. The Napa River also flows into Carquinez Strait from the north, at the entrance to the larger San Pablo Bay. The deeper Central Bay, followed by South Bay, is located to the south of San Pablo Bay. The complete Bay system covers a surface area of approximately 1219 km^2 at MSL. The median water depth is 3.6 m relative to mean sea level. Tide range is about 1–3 m depending on the spring/neap tidal cycle and location in the Bay. Winds are strongest in the spring and summer and re-suspend sediment in water less than about 2 to 3 m deep (Ruhl and Schoellhamer, 2004).

The San Francisco Bay area has a long history with sediment transport and flocculation research, dating back to the classic work of H.A. Einstein, R.B. Krone and E. Partheniades (e.g. Einstein, 1941; Einstein and Krone, 1962; Krone, 1962; Partheniades, 1962; Krone, 1963, 1986). This interest in SFB sediments originates back to the anthropogenic events of the mid-nineteenth century. During the last 160 years, the bathymetry and sedimentation within the Bay have undergone many evolutions, primarily due to anthropogenic input. These included vast amounts of mud and gravel sediments being released initially into the upper reaches of the Sacramento River during hydraulic mining activities in the 1850s (Gilbert, 1917), followed by the reclamation of wetlands which was carried out from the mid 1800s to the late 1900s. This activity has had the net effect of reducing San Francisco Bay's original size by about one third. Schoellhamer et al. (2007) provide an overview of how suspended sediment concentrations (SSCs) are distributed throughout San Francisco Bay and the correlation between SSC and sediment-adsorbed contaminants.

The bottom sediments in South Bay and in the shallow water areas (about 3 m or less) of Central, San Pablo, and Suisun Bays are composed mostly of silts and clays. Silts and sands are present in the deeper parts of Central, San Pablo, and Suisun Bays and in Carquinez Strait (Conomos and Peterson, 1977). Krone (1962) conducted laboratory experiments and found that settling velocity was proportional to $SSC^{4/3}$ when SSC > 300 $mg \cdot l^{-1}$, a relation widely used in many estuaries. Kineke and Sternberg (1989) found that flocs in San Pablo Bay commonly had a diameter of about 100 μm and had a settling velocity of 0.5 to 2.0 $mm \cdot s^{-1}$. Kranck and Milligan (1992) found that the population of small flocs remained fairly constant through a tidal cycle in San Pablo Bay but the number of large flocs increased as the SSC increased. Based on measurements of mass and volume concentration, Ganju et al. (2007) found that the relation between floc diameter and floc density was constant throughout San Francisco Bay, which implies that primary particle size, fractal dimension, and flocculation mechanisms are homogeneous.

3. Methods and materials

Since 1968, to chart long term changes in water quality, the U.S. Geological Survey has been making approximately monthly water quality cruises along the longitudinal axis of San Francisco Bay from South Bay north then east to the Sacramento River (http://sfbay.wr.usgs.gov/access/wqdata/). The transect commenced in South Bay near the *USGS Reference Station 36#* on June 17th, 2008 and comprised 35 stations spaced 3–6 km apart (see Fig. 1). The cruise is predominantly La Grangian, following the flood tide progress inland, but with data being collected at each station in a quasi-Eulerian manner. Samples were collected at each station in one day. The Research Vessel *Polaris* was brought close to stationary at each sampling station and remained on station, unanchored, for approximately 5–10 min (the duration was dependent upon the number of devices being deployed and the total water depth at each site).

Flocs, although stable in flowing turbulent water, easily break apart when sampled in response to additional shear created during acquisition (Eisma et al., 1997). Therefore, the floc data were primarily acquired using the INSSEV-LF: IN-Situ Settling Velocity instrument. The LF (LabSFLOC) version of INSSEV is a hybrid system which combines two key components: i) the low intrusive LabSFLOC system (a high resolution video-based device to measure the individual floc properties; ii) an in-situ estuarine floc sampling acquisition unit (to initially obtain the suspension sample). For the latter, a 2.2 l Van Dorn horizontal sampling tube with a 14 kg torpedo-shaped weight suspended from the underside of the tube was used to collect a water sample nominally 0.7 m above the estuary bed. Manning et al. (2010) provide further details of the floc acquisition procedures.

The LabSFLOC – Laboratory Spectral Flocculation Characteristics – instrument (Manning, 2006) was set up in the fan-tail section at the vessel's stern. It utilises a low-intrusive high magnification analogue video camera (Manning and Dyer, 2002) to observe flocs as they settle in a 190 mm high by 100 mm square Perspex settling column. The LabSFLOC camera resolution could practically view flocs down to 20 μm in size and as large as 4 mm. Settling velocities generally ranging from 0.01 $mm \cdot s^{-1}$ to 35 $mm \cdot s^{-1}$ can be measured by LabSFLOC. Similarly, INSSEV can operate within SSCs of just a few $mg \cdot l^{-1}$, with a practical upper operating limit of ~8.5 $g \cdot l^{-1}$.

A small sub-sample containing a floc population was carefully extracted from the horizontal Van Dorn using a modified pipette. This sample was immediately transferred to the LabSFLOC settling chamber, whereby the flocs passed from the vertically held pipette to the chamber and settled solely under gravity. The floc collection and sub-sampling protocol are both proven floc sampling techniques (see Manning, 2006; Mehta et al., 2009; Manning et al., 2010), which permit minimal floc interference and flocs which are representative of the ambient population — especially in terms of floc size and settling velocity distributions. The floc sampling techniques also provide control volumes, which permit settling flux estimations.

A dual-axis spirit level was attached to the settling column, which enabled the constant monitoring of the verticality of the settling column whilst on the survey vessel. The video camera utilises a back-illumination system, provided by an annulus of six high intensity red 130 mW LEDs positioned around the camera lens, whereby floc images are silhouettes i.e. particles appear dark on a light background. The settling column was shaded from bright sunlight during the survey.

Additional floc data was obtained through vertical profiles of particle size data and volume concentration using a LISST-100[1] instrument (deployed from mid-ships on the port side). This is an autonomous instrument that measures laser diffraction from suspended particles, and assigns each particle to 1 of 32 logarithmically spaced size classes (1–250 μm; Agrawal and Pottsmith, 1994). It estimates the volume of a floc by using the small-angle scattering of the laser beam; this is known as Mie theory (Mie, 1908; Xu, 2000) which is an analytical solution of Maxwell's equations (see Stratton, 1941) for the scattering of electromagnetic radiation by small spheres. The output of the LISST-100 is total volume concentration (μl/l) in each size class.

Vertical profiles of salinity, temperature, chlorophyll, suspended particulate matter were collected using a SBE 19-03 CTD SEACAT Profiler. Niskin bottle water samples (for gravimetric analysis) were also collected at some stations to calibrate instruments.

4. Data analysis

4.1. Floc data

LabSFLOC digitises the analogue grey-scale floc images via a Zarbeco USB-2.0 Videolink PC card. The images were digitised during post-processing after the survey, at a frame rate of 25 Hz (one frame = 0.04 s), at a resolution of 640 × 480 pixels, with an individual pixel representing 6.3 μm (determined from calibration). A typical floc image was deemed to comprise of at least three linked pixels, resulting in a practical lower floc resolution ~20 μm. Each floc video image time series is converted into separate AVI format files (one for each floc sample). The AVI files were not codec compressed, so they could be analysed with MatLab software routines during post-processing. This meant that each 360 s AVI file was approximately 4.2 GB in size; therefore all AVI files were recorded to a USB-2.0 portable 1 TB hard drive.

The HR Wallingford Ltd *DigiFloc* software — version 1.0 (Benson and Manning, in press), was then used to semi-automatically process the digital floc image recordings to obtain D and Ws spectra. By measuring both the major-axis and minor-axis of each observed two-dimensional floc image, a spherically equivalent floc diameter

[1] Any use of trade, product, or firm names is for descriptive purposes only and does not imply endorsement by the U.S. Government.

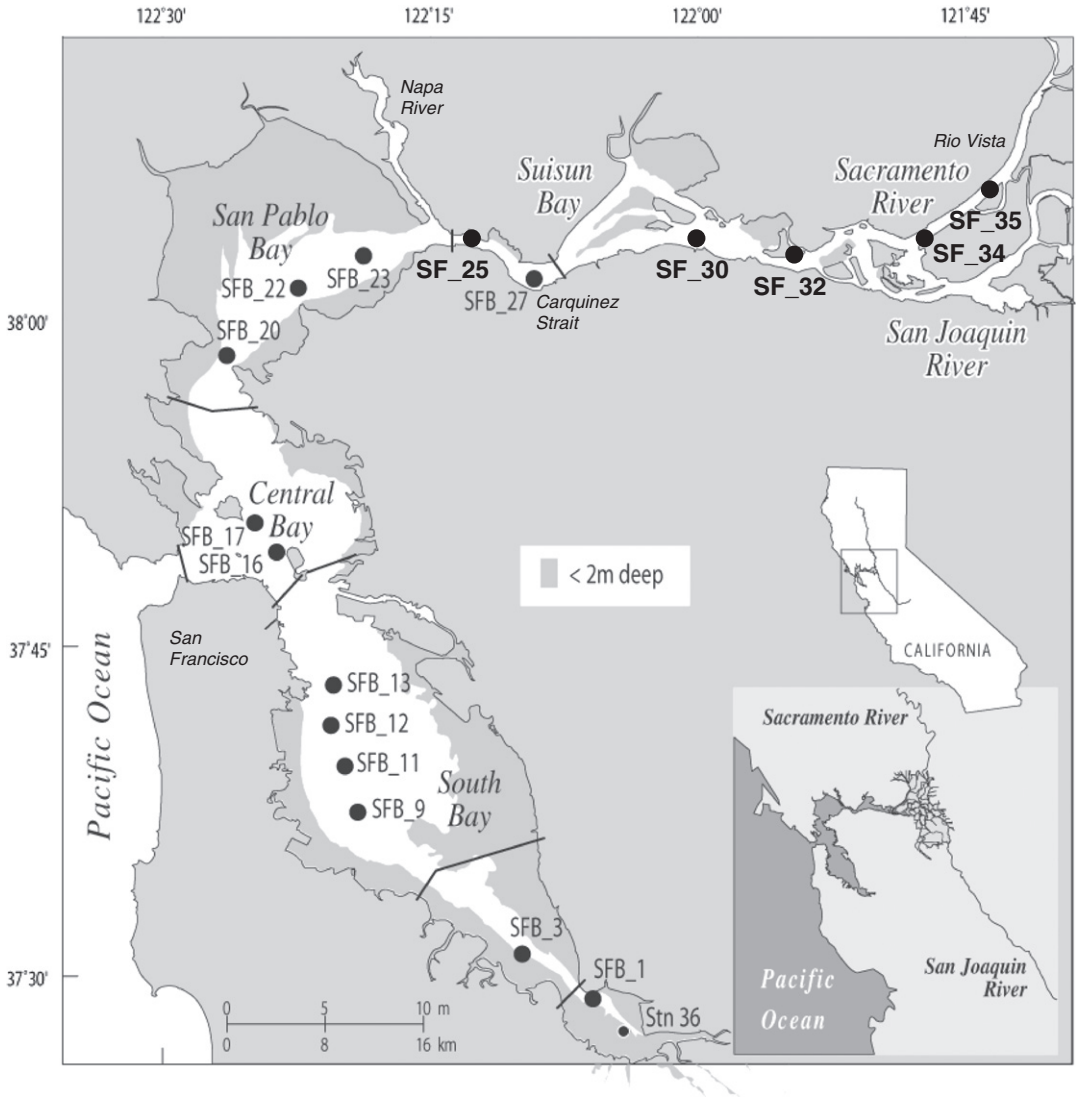

Fig. 1. San Francisco Bay system, including a selection of the 35 sampling stations. Note the location of the USGS Reference Station 36# in South Bay, from which all transect distances are taken.

(D) could be determined from: $D = (D_{major} \cdot D_{minor})^{0.5}$. Effective or submerged floc densities were calculated from the measured diameter and settling velocity with Stokes equation:

$$\rho_e = \rho_f - \rho = \frac{18 Ws \mu}{g D^2} \quad (1)$$

in which ρ_f is the floc bulk density, ρ the is the fluid density, Ws is the settling velocity, μ is the molecular viscosity, g is gravitational acceleration, and D is the diameter (Garcia, 2007). The floc effective density, ρ_e, is calculated by subtracting the water density from the floc bulk density. When the Reynolds number $Re = \rho_e Ws \cdot D / \mu > 0.5$, the right hand side of Eq. (1) is multiplied by Oseen's (1927) correction factor $1 / (1 + 0.1875 * Re)$ to account for turbulence.

As a result of measuring all visible flocs within an individual LabSFLOC sample and by assuming the flocs originated from a constant sample volume of water, 400 mm^3 (defined by: a 4 mm image width, a 1 mm camera depth-of-field and 100 mm volume height), it is possible to transform the observed floc population into accurate estimates of SSC and settling flux spectra. Using specially derived algorithms (Fennessy et al., 1997; Manning, 2004b), it was possible to accurately calculate other physical characteristics for each individual floc, including: porosity and dry mass.

The mass settling flux (MSF) of suspended sediment is the product of settling velocity and mass concentration, and can provide an indication of depositional rates. For each INSSEV-LF floc population, the sample MSF was calculated by summing the product of each individual floc fall velocity and its respective contribution to the SSC. Flocs with relatively little mass contribute little to the settling flux whilst more massive flocs contribute more. This approach provides both a highly accurate representation of both the total MSF and quantitative information of how the flocs contribute to the MSF across a floc population.

To aid in the interpretation of the floc characteristics (e.g. D, Ws), each floc population was segregated into various sub-groupings based on floc size. As with many previous studies on flocculation, the sample mean floc values were computed (i.e. a single value per floc population) to show generalised floc property trends (e.g. mean settling velocity is Ws_{mean} and maximum settling velocity is Ws_{max}). In order to provide a single settling characteristic for a population of flocs in a water sample, which represented the mass variability to a better degree than the basic Ws_{mean}, the mass-weighted settling velocity Ws_{mass} parameter was calculated as:

$$Ws_{mass} = \frac{\sum_t \rho_{fi} w_{si} d_1^3}{\sum_i \rho_{fi} d_i^3}. \quad (2)$$

In accordance with numerous flocculation modelling studies, flocs were also assessed in terms of macrofloc (e.g. Ws_{macro}) and microfloc (e.g. Ws_{micro}) sub-populations. Manning (2001) classifies macroflocs as those aggregates which exceed a spherically equivalent diameter of 160 μm, whereas the microflocs D < 160 μm. This macrofloc:microfloc parameterisation produces two floc property values per floc population.

4.2. Hydrodynamics

Water turbulence during the cruise was not directly measured, so we use the depth-averaged current speed as a surrogate to estimate turbulence and shear stress parameters in the nearbed region. This assumption neglects turbulence damping by vertical stratification. To estimate the effect of tidal currents on the floc data, depth-averaged current speed (u) at sampling stations was calculated using the UnTRIM three-dimensional numerical model which was calibrated to data from San Francisco Bay by MacWilliams et al. (2008, also discussed by Kimmerer et al., 2009). The model was run with a 3-min time step through June 17th 2008, and vertical velocity profiles and depth-averaged current speed at the locations of cruise sampling were extracted.

Using the mean flow velocity parameter (u), the nearbed frictional (shear) velocity U_* was calculated by (Delo, 1988):

$$U_* = u \cdot ng^{-1}/H^{1/6} \quad (3)$$

where: n is Manning's bed roughness coefficient, g is acceleration due to gravity, and H is the nominal depth of flow. Appropriate values of n as a function of H were recommended by Cheng et al. (1993) for SFB.

The average local shear stress (τ), with the units Pa, was calculated from:

$$\tau = \rho_w U_*^{\mathbf{2}}. \quad (4)$$

In addition, two commonly used turbulence parameters were calculated. The first was the root mean square of the gradient in turbulent velocity fluctuations (G), with the units of s^{-1}:

$$G = 4.34(U_*/\upsilon \cdot H)^{0.5} \quad (5)$$

where υ is the kinematic viscosity. Eq. (5) is valid for measurements within the 0.1 H region close to the sea bed (van Leussen, 1997).

The second parameter classifies the turbulence level by the size of the dissipating eddies as defined by Kolmogorov (1941a,b), and is referred to as the microscale of turbulence η (units are μm):

$$\eta = (\upsilon/G)^{0.5}. \quad (6)$$

5. Results

A total of 30 floc samples were collected at a nominal height of 0.7 m above the estuary bed during the SFB survey on June 17th 2008 from the 35 stations visited (strong sunlight compromised the image quality of flocs viewed at five locations). During the transect a combined total of 4346 individual flocs were measured. All transect distances (given in km) are zero referenced to *USGS Reference Station 36#* in South Bay (see Fig. 1). Table 1 provides a summary of the sampling stations, distances along the transect and data acquisition times.

The corresponding hydrodynamic parameters are illustrated in Fig. 2 and summarised in Table 2. Predicted depth-averaged flow velocities peaked at 0.88 $m \cdot s^{-1}$, with a transect cruise average of 0.52 $m \cdot s^{-1}$. The highest nearbed shear stress of 0.82 Pa ($G = 66\ s^{-1}$) occurred just after high water in the Chain Island region and these high turbulence conditions reduced the Kolmogorov microscale to 123 μm ($G = 66.5\ s^{-1}$). Low water slack in South Bay produced the least turbulent conditions of the cruise, with a large Kolmogorov microscale of 1.4 mm ($\tau = 0.01$ Pa and $G = 0.5\ s^{-1}$). The transect average turbulent shear stress τ_{mean} was 0.33 Pa, with corresponding $G_{mean} = 38.5\ s^{-1}$ and $\eta_{mean} = 259$ μm.

5.1. Longitudinal observations

5.1.1. Overview

The floc settling velocity distribution was consistent for most of the stations and median Ws_{mass} was 5.3 $mm \cdot s^{-1}$ and the inter-quartile range was 2.5–6.4 $mm \cdot s^{-1}$ (Fig. 3). The transect started in South Bay towards the end of ebb tide, with slack tide occurring when the *RV Polaris* was about 16 km into the transect. The tide turned to flood and remained flooding for the remainder of the transect. Settling velocities were much smaller (typically Ws_{mass} of 1–2 $mm \cdot s^{-1}$) in South Bay 60–90 min after slack tide in the vicinity of San Bruno Shoal, a large sandy deposit. Faster settling sediment deposited during slack, leaving only slowly settling sediment in suspension. Although the non-slack distributions of settling velocity appear similar, they are not statistically from the same population (Kruskal–Wallis test). Mass-weighted settling velocity Ws_{mass} generally was between the median and upper quartile of individual floc settling velocities because less massive flocs usually settled slower than more massive flocs.

Salinity was nearly homogeneous in South and Central Bays and decreased to zero landward in North Bay. SSC had maxima in lower South Bay, probably due to wind wave resuspension on intertidal flats, and at the estuarine turbidity maximum in Carquinez Strait (Schoellhamer, 2001).

5.1.2. Time series details

In order to investigate the longitudinal evolution in the floc properties, time series of the sample mean and macrofloc:microfloc parameterised floc properties have been plotted in Fig. 4, together with the variations in salinity and SSC, all at the nominal INSSEV-LF acquisition height (0.7 m above the estuary bed).

The SFB survey on June 17th 2008 commenced two hours before low water (LW; 06:17 h) from the southern tidal limit of South Bay (3.5 km). In terms of local classification, South Bay is representative of a tidal lagoon (salinity = 27 at the estuary bed; Fig. 4a) and has a mean low water (MLW) depth ranging from 7.5–15 m. Initially the SSC in South Bay was 230 $mg \cdot l^{-1}$ at Newark Slough (Fig. 4a), which was the peak encountered during the survey and $\tau = 0.24$ Pa ($G = 21.7\ s^{-1}$ and $\eta = 213$ μm). The early South Bay turbidity at SFB_1 was too high for the LISST-100 to operate (Fig. 4b). The INSSEV-LF data showed the abundance of fine-grained cohesive sediment created the D_{mean} of 170 μm for SFB_1, with a corresponding Ws_{mean} of 4.4 $mm \cdot s^{-1}$ (Fig. 4c). However the individual population distribution indicates that individual flocs 584 μm in diameter were present in SFB_1 (see Fig. 5a), and this was reflected in the macrofloc fraction (D > 160 μm) comprising 61% of the floc mass (Fig. 4d) and settling at a Ws_{macro} of 5.4 $mm \cdot s^{-1}$, which was 1 $mm \cdot s^{-1}$ quicker than the sample average (see Fig. 4e).

A phytoplankton bloom was visually observed in the vicinity of Dumbarton Bridge (SFB_2; 7 km), and both the SSC and turbulent shear stress ($\tau = 0.043$ Pa, $G = 7.3\ s^{-1}$ and $\eta = 367$ μm) began to quickly decrease by an order of magnitude. Approaching slack LW ($U \sim 0.03–0.1\ m \cdot s^{-1}$), the SSC fell to ~30 $mg \cdot l^{-1}$ north of San Mateo Bridge (26 km). With a reduction in the bed shear stress, the faster settling macroflocs which were earlier present in the water column, had now deposited to the bed, leaving just small microflocs in suspension. This was reflected in 62% of the SSC present as microflocs in sample SFB_9 ($\tau = 0.11$ Pa), and both microfloc and macroflocs demonstrating similar slow fall rates of 0.6 $mm \cdot s^{-1}$. With only 8 of the 97 flocs larger than 200 μm (see Fig. 5c), the $D_{mean} = 114$ μm, although this was significantly larger than the corresponding D_{50} of 26 μm from the LISST.

Table 1
Summary of the sampling times (PDT), floc sample references, station details, distances along the transect and nominal LW depths.

Sample time (h; PDT)	Floc sample (SB_**)	USGS site (#)	Location name	Latitude (north)	Longitude (west)	Distance from USGS Reference Station 36# (km)	Depth at mean LW (m)
06:17	1	34	Newark Slough	37° 29.7′	122° 5.6′	3.5	7.9
06:35	2	33	Dumbarton Bridge	37° 30.5′	122° 7.3′	6.8	11.6
06:45	3	32	Ravenswood Point	37° 31.1′	122° 8.0′	8.2	12.8
06:55	–	31	Coyote Hills	37° 31.7′	122° 9.5′	10.6	13.7
07:15	5	30	Redwood Creek	37° 33.3′	122° 11.4′	14.8	12.8
07:28	–	29.5	Steinberger Slough (ns)	37° 34.1′	122° 13.1′	17.6	14.6
07:40	–	29	S. of San Mateo Bridge	37° 34.8′	122° 14.7′	20.3	14.6
07:55	8	28	N. of San Mateo Bridge	37° 36.1′	122° 16.2′	23.6	16.2
08:12	9	27	San Francisco Airport	37° 37.1′	122° 17.5′	26.2	13
08:27	–	26	San Bruno Shoal	37° 38.1′	122° 18.8′	28.8	9.8
08.45	11	25	Oyster Point	37° 40.2′	122° 19.5′	32.8	8.8
09.00	12	24	Candlestick Point	37° 41.9′	122° 20.3′	37.1	11
09:20	13	23	Hunter's Point	37° 43.7′	122° 20.2′	39.7	20.1
09:40	14	22	Potrero Point	37° 45.9′	122° 21.5′	43.9	18
10:00	15	21	Bay Bridge	37° 47.3′	122° 21.5′	46.6	17.4
10:25	16	20	Blossom Rock	37° 49.2′	122° 23.6′	51.5	18.2
10:50	17	18	Point Blunt	37° 50.8′	122° 25.3′	55.0	43
11:05	18	17	Raccoon Strait	37° 52.9′	122° 25.6′	58.9	32
11:25	19	16	Charlie Buoy	37° 54.9′	122° 26.8′	63.1	43
11:47	20	15	Point San Pablo	37° 58.5′	122° 26.2′	70.0	22.9
12:05	21	14	Echo Buoy	33° 0.4′	122° 24.3′	74.4	131
12:18	22	13	N. of Pinole Point	38° 1.7′	122° 22.2′	78.5	9.8
12:40	23	12	Pinole Shoal	38° 3.1′	122° 18.7′	84.5	8.8
12:55	24	11	Mare Island	38° 3.7′	122° 15.8′	89.8	15.5
13:15	25	10	Crockett	38° 3.6′	122° 12.5′	93.6	17.7
13:30	26	9	Benicia	38° 3.0′	122° 10.4′	96.8	34.4
13:45	27	8	Martinez	38° 1.8′	122° 9.1′	99.8	14.3
14:10	28	7	Avon Pier	38° 2.9′	122° 5.8′	105.0	11.6
14:30	29	6	Roe Island	38° 3.9′	122° 2.1′	110.9	10.1
14:50	30	5	Middle Ground	38° 3.6′	121° 58.8′	115.6	9.8
15.07	31	4	Simmons Point	38° 2.9′	121° 56.1′	119.9	11.6
15:30	32	3	Pittsburgh	38° 3.0′	121° 52.7′	125.3	11.3
15:52	–	2	Chain Island	38° 3.8′	121° 51.3′	127.7	11.3
16:14	34	649	Sacramento River	38° 3.7′	121° 48.0′	132.9	10.1
17:03	35	657	Rio Vista	38° 8.9′	121° 41.3′	147.3	10.1

The SFB_9 macrofloc fraction had a mean effective density of just 27 $kg \cdot m^{-3}$ (see Fig. 4f), which suggests they were extremely fragile and possibly organically-based flocs; over 98% porous. The ρ_{e_micro} (239 $kg \cdot m^{-3}$) was an order of magnitude greater than the SFB_9 ρ_{e_macro} (27 $kg \cdot m^{-3}$). If we compare these density values to SFB_1, we can see that the ρ_{e_micro} of 851 $kg \cdot m^{-3}$ is significantly higher, whilst the SFB_1ρ_{e_macro} (164 $kg \cdot m^{-3}$) is more indicative of the microfloc density in the vicinity of the San Mateo Bridge. This suggests that the macrofloc and microflocs may have different compositional matrices at different locations throughout SFB; this will be discussed in Section 6.

The nf_{macro} (see Fig. 4g) generally ranges between 2.4 and 2.6, with the main exception being SFB_9 where the macrofloc fractal dimension dips below 2. The nf_{micro} near the San Mateo Bridge was also quite low (~2.2). Overall the microflocs demonstrated a much wider range in fractal dimension (than the macroflocs) throughout SFB, peaking at an nf_{micro} approaching 3 in the marine conditions of Central Bay (SFB_17 and SFB_18).

The flood current speed started to increase (U = 0.6–0.8 $m \cdot s^{-1}$) during the last 10 km of South Bay and then on entering the deeper Central Bay (~55 km; MLW depth of 18–43 m) between LW + 2:30 h and LW + 3:45 h. This caused the turbulent shear stresses to rise (τ = 0.45–0.67 Pa). The turbidity dipped to the lower end of the transect scale in Central Bay, with an SSC of just 21 $mg \cdot l^{-1}$ for sample SFB_17 (Point Blunt) where the τ was 0.31 Pa (G = 66.3 s^{-1} and η = 121 μm). The microflocs were dominating 73% of the floc mass, and Ws_{micro} was only 0.06 $mm \cdot s^{-1}$ slower than the Ws_{macro} of 5.1 $mm \cdot s^{-1}$. Again the macro- and microfloc fractions exhibit very different effective densities; over 900 $kg \cdot m^{-3}$ separating the two fractions, with the denser ρ_{e_micro} = 1068 $kg \cdot m^{-3}$. Both the LISST D_{50} and INSSEV-LF indicated an average floc diameter of 104 μm (±4 μm).

On entering San Pablo Bay (Point San Pablo; 70 km), the salinity stratification (27 at the estuary bed) started to become more apparent, when compared to the predominantly marine conditions (salinity of 32 at the seabed) of the Central Bay. The mean current speed was 0.85 $m \cdot s^{-1}$ and τ = 0.57 Pa (G = 78 s^{-1} and η = 112 μm). The D_{mean} rose to 200 μm (SFB_20); a similar mean size observed by INSSEV-LF at the start of the transect, but now demonstrate a 1.2 $mm \cdot s^{-1}$ quicker fall rate (Ws_{mean} = 5.6 $mm \cdot s^{-1}$). Again the denser microflocs were settling (Ws_{micro} of 5.4 $mm \cdot s^{-1}$; ρ_{e_micro} of 888 $kg \cdot m^{-3}$) at a comparable rate to the more porous, macroflocs. This similarity in fall rates could be a function of the skeletal floc sediment comprising the different floc matrices being a combination of organic muds mixed with denser fine marine sands. This mixed sediment flocculation issue will be discussed in Section 6.

The turbidity maximum zone (TMZ) was observed at Carquinez Strait (99.8 km; Benicia and Martinez) around high water, a feature of this region of San Francisco Bay (Schoellhamer, 2001). The mean flow speed was 0.75 $m \cdot s^{-1}$ and τ = 0.49 Pa (G = 57 s^{-1} and η = 132 μm). The LISST-100 observations (Fig. 4b) indicate a D_{50} floc size of 144 μm within the TMZ, just 4 μm smaller than the INSSEV-LF D_{mean}. The near bed SSC within the TMZ was ~161 $mg \cdot l^{-1}$, and near bed salinity was 15. TMZ conditions produced some of the largest flocs observed during the cruise with D exceeding 400 μm (see Fig. 5g) and these flocs (SFB_27) will be examined in greater detail in the next section.

On entering Suisun Bay (SFB_28 at 105 km; Avon Pier), there was a noticeable decrease in SSC and U had slowed by 0.17 $m \cdot s^{-1}$; both a result of the natural sill present at the easterly end of Carquinez Strait.

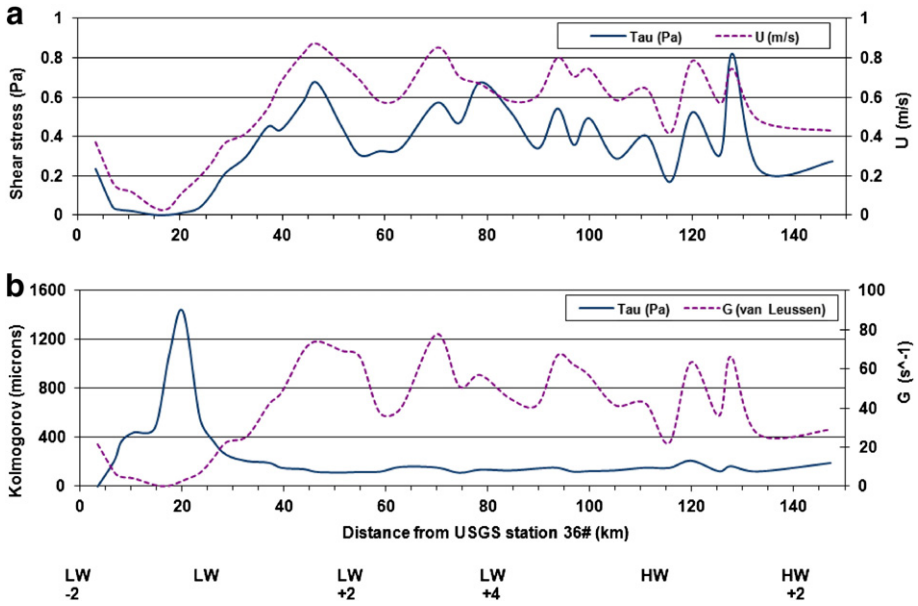

Fig. 2. Time series illustrating the longitudinal variation of the estimated hydrodynamic parameters in SFB: a) depth-average current velocity and nearbed turbulent shear stress, b) nearbed G turbulence parameter (from van Leussen, 1994) and Kolmogorov eddy microscale size. The distance from USGS Reference Station 36# and relative tidal state are both indicated on the y-axis.

Salinity was now only 12. The combined reduction in suspended sediment and a 0.2 Pa fall in turbulent shear stress ($\tau = 0.29$ Pa) brought about a marked reduction in flocculation, when compared with the TMZ flocs. Macroflocs now only comprised 16% of the suspended sediment at the less turbid (SSC = 87 mg·l^{-1}) Avon Pier, whereas more than half the SSC within the TMZ were macroflocs. In terms of floc dynamics, the SFB_28 D_{mean} was only half the mean floc size observed in Carquinez Strait. Similarly the Ws_{mean} had slowed by

Table 2
Summary of estimated hydrodynamic parameters.

Sample time (h; PDT)	Floc sample (SB_**)	USGS site (#)	Distance from USGS Reference Station 36# (km)	Predicted depth-averaged current velocity u (m/s)	U* (m/s)	τ (Pa)	G (s^−1)	Kolmogorov (microns)
06:17	1	34	3.5	0.372	0.015	0.236	21.7	213
06:35	2	33	6.8	0.169	0.006	0.043	7.3	367
06:45	3	32	8.2	0.134	0.005	0.028	5.0	442
06:55	–	31	10.6	0.118	0.005	0.021	4.2	480
07:15	5	30	14.8	0.041	0.002	0.003	0.8	1076
07:28	–	29.5	17.6	0.032	0.001	0.001	0.5	1433
07:40	–	29	20.3	0.111	0.003	0.012	3.1	558
07:55	8	28	23.6	0.19	0.006	0.035	7.0	373
08:12	9	27	26.2	0.269	0.010	0.110	14.6	259
08:27	–	26	28.8	0.368	0.014	0.213	22.7	207
08:45	11	25	32.8	0.418	0.017	0.298	25.8	195
09:00	12	24	37.1	0.545	0.021	0.451	42.1	152
09:20	13	23	39.7	0.68	0.021	0.435	48.5	142
09:40	14	22	43.9	0.822	0.024	0.575	69.6	118
10:00	15	21	46.6	0.875	0.026	0.676	74.3	115
10:25	16	20	51.5	0.774	0.021	0.453	69.4	119
10:50	17	18	55.0	0.692	0.017	0.308	66.3	121
11:05	18	17	58.9	0.581	0.018	0.326	37.6	161
11:25	19	16	63.1	0.603	0.018	0.342	40.5	155
11:47	20	15	70.0	0.854	0.024	0.572	78.0	112
12:05	21	14	74.4	0.707	0.021	0.469	51.4	138
12:18	22	13	78.5	0.669	0.026	0.677	57.1	131
12:40	23	12	84.5	0.581	0.023	0.527	44.9	148
1255	24	11	89.8	0.61	0.018	0.340	41.8	153
13:15	25	10	93.6	0.803	0.023	0.544	66.9	121
13:30	26	9	96.8	0.707	0.019	0.358	62.4	126
13:45	27	8	99.8	0.745	0.022	0.494	57.2	132
14:10	28	7	105.0	0.587	0.017	0.289	41.7	154
14:30	29	6	110.9	0.646	0.020	0.406	42.8	152
14:50	30	5	115.6	0.419	0.012	0.110	22.3	211
15:07	31	4	119.9	0.788	0.023	0.525	63.7	125
15:30	32	3	125.3	0.571	0.017	0.307	36.2	166
15:52	–	2	127.7	0.746	0.029	0.823	66.5	123
16:14	34	649	132.9	0.483	0.015	0.232	27.0	193
17:03	35	657	147.3	0.431	0.017	0.274	29.2	185

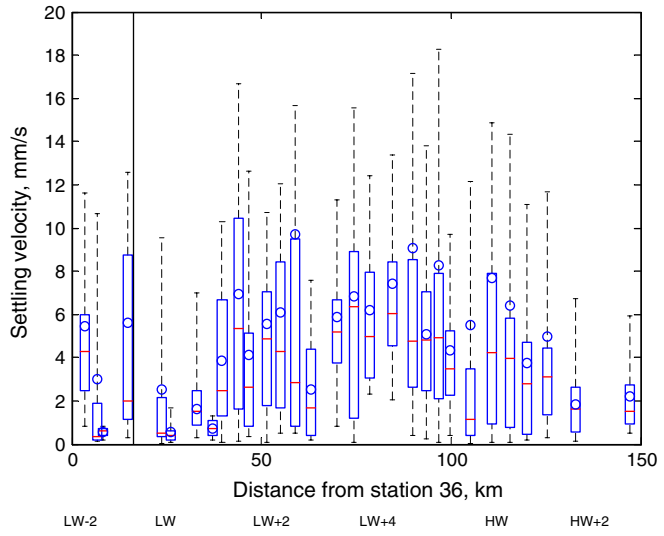

Fig. 3. Distribution of settling velocity and mass-weighted settling velocity along the longitudinal transect. Each box plot indicates maximum settling velocity (upper dash), upper quartile (top of box), median (line in box), lower quartile (bottom of box), and minimum (lower dash). Circles indicate mass-weighted settling velocity Ws_{mass}. The vertical dashed line indicates the time of slack tide in South San Francisco Bay. Sampling location relative to times of low water (LW) and high water (HW) are indicated.

1.3 $mm \cdot s^{-1}$ to 2.4 $mm \cdot s^{-1}$ from the average fall rate measured previously within the TMZ.

The cruise concluded midway through the afternoon ebb at Rio Vista (SFB_35; 147 km) on the Sacramento River, where the river was ebbing at a velocity of 0.43 $m \cdot s^{-1}$ and producing a τ of 0.27 Pa ($G = 29\ s^{-1}$ and $\eta = 185$ μm). The water column was now fully fresh and the SSC was 35 $mg \cdot l^{-1}$. The LISST-100 suggested a D_{50} of just 33 μm, which was just one quarter of the mean floc diameter measured by the INSSEV-LF. This highlights how different instruments can see the same ambient floc population in a different way. The mean fall rate was now less than 2 $mm \cdot s^{-1}$ and microflocs dominated this freshwater environment ($SSC_{micro} = 68\%$).

The total mass settling fluxes measured at each of the stations are illustrated in Fig. 4h. The very turbid southerly South Bay (SFB_1) produced a transect peak MSF of over 1.1 $g \cdot m^{-2}\ s^{-1}$, which was nearly double the flux observed in the TMZ (SFB-27). Settling fluxes seaward of Dumbarton Bridge (in South Bay) ranged from 11 $mg \cdot m^{-2}\ s^{-1}$ (SFB_3) to 307 $mg \cdot m^{-2}\ s^{-1}$ at Hunter's Point (SFB_13). MSFs ranged from 31–160 $mg \cdot m^{-2}\ s^{-1}$ within the marine environment of Central Bay. As the transect entered San Pablo Bay, the settling fluxes steadily rose and by Pinole Shoal (SFB_23; 84.5 km) the MSF had doubled in magnitude to 319 $mg \cdot m^{-2}\ s^{-1}$ (when compared to the peak MSF observed in Central Bay).

Mass settling fluxes observed in Suisun Bay (SFB_28–31; MSF range: 178–303 $mg \cdot m^{-2}\ s^{-1}$) were comparable to the higher end of the MSF values measured in San Pablo Bay. It was noted earlier that microflocs dominated the floc populations in Suisun Bay and this had the result of producing a MSF at SFB_28 which was only 40% of the settling flux observed within the TMZ (MSF in Carquinez Strait at SFB_27 = 633 $mg \cdot m^{-2}\ s^{-1}$). Settling fluxes reduced as the transect entered the Sacramento River, falling to 72 $mg \cdot m^{-2}\ s^{-1}$ at Rio Vista (SFB_35).

5.2. Floc size and settling velocity distributions

To illustrate the floc population dynamics throughout the transect, nine populations ('9#' indicates various combined totals for all nine samples) were selected as providing representative floc population characteristics at the various sampling zones throughout the transect. The first three samples selected (SFB_1, 3 and 9; Fig. 5a–c) were obtained from South Bay, which is predominantly a tidal lagoon. Sample SFB_17 (Fig. 5d), followed by SFB_20 and SFB_22 (Fig. 5e–f) was acquired from the more marine environments of Central Bay and San Pablo Bay, respectively. SFB_27 (Fig. 5g), was collected in the brackish waters of Carquinez Strait within the estuary TMZ, and SFB_28 (Fig. 5h) was in Suisun Bay. Our final example was from the latter part of the transect in the Sacramento River (SFB_35; Fig. 5h) at Rio Vista.

The nine floc populations are shown in Fig. 5. The scatterplots illustrate individual spherical-equivalent dry mass weighted floc sizes (x-axis) plotted against their corresponding settling velocities (y-axis) for each sample. The nine floc populations comprised a total of 1761 individual flocs (to provide a mass-balance within the 400 mm^3 reference sample volume), 30% of which were over 160 μm in diameter. Although the macroflocs were less abundant, they contained 40% of the total floc mass for 9# and 58% of the mass settling flux (MSF for $9^{\#} = 2.74\ g \cdot m^{-2}\ s^{-1}$) due to their quicker settling velocities.

The 9# experimental conditions produced individual flocs ranging in size from 24 μm microflocs (SFB_28) to 639 μm macroflocs (SFB_1) — all single point sizes. The 9# single point settling velocities ranged from 0.04 to 0.08 $mm \cdot s^{-1}$ (SFB_9 and SFB_28) at the slower end; quickening to Ws of 12.5–15.8 $mm \cdot s^{-1}$ (SFB_1, SFB_17 and SFB_22).

The diagonal lines on Fig. 5 scatterplots represent contours of constant floc effective density (i.e. floc bulk density minus the water density; units = $kg \cdot m^{-3}$). From a visual inspection of Fig. 5, one can see that the majority of the San Francisco Bay floc densities spanned three orders of magnitude. Typically the floc effective densities varied from fragile, highly porous (>99%), low density flocs with ρ_e of 2–9 $kg \cdot m^{-3}$ (e.g. SFB_9), to the less porous (20–45%) microflocs which exhibit ρ_e up to 700–1000 $kg \cdot m^{-3}$. One can see that there are many flocs of different sizes, but exhibiting a similar floc density. Also there are flocs present with similar settling velocities, but demonstrating a wide range of sizes and effective densities.

Individual sand grains were present in a number of locations, in particular Central Bay (SFB_17), and are indicated by clustering around the pink contour lines on Fig. 5, which is representative of a pure quartz grain with a ρ_e of 1600 $kg \cdot m^{-3}$. A few small unflocculated particles were exhibiting effective densities beyond 2000 $kg \cdot m^{-3}$. These are most probably either denser sedimentary facies and/or microscopic fragments of a metallic composition (e.g. anthropogenically deposited in the Bay as a result of shipping, etc.). However these high density particles were in the minority; comprising less than 1.5% of all the 9# flocs observed. These high density particles have been retained in the data set, as other high density particles may have been incorporated into the matrix of other flocs observed during the transect.

The peak transect SSC (230 $mg \cdot l^{-1}$) was encountered in South Bay (SFB_1; Fig. 5a) and comprised a population of 522 individual flocs, 299 of which were microflocs. The scatterplot spanned the widest size range (611 μm) of all thirty floc samples collected during the transect. The effective density of the flocs less than 100 μm in diameter were all great than 160 $kg \cdot m^{-3}$. Once the macroflocs grew beyond 300 μm, their $\rho_e < 160\ kg \cdot m^{-3}$. In fact the eighteen flocs larger than 500 μm, just 3.5% of the total population, predominantly demonstrated $\rho_e < 30\ kg \cdot m^{-3}$ (porosity > 98.5%; nf ~2.2), but Ws of 3–8 $mm \cdot s^{-1}$. Thus, this fragile, large size fraction represented over 10% of both the ambient SSC and total MSF (1.1 $g \cdot m^{-2}\ s^{-1}$).

The longitudinal data presented in Fig. 4 suggested a distinct variation in floc properties throughout the SFB system. If for example we consider Central Bay (Fig. 5d), we can see that the population comprises 70 flocs, 61 of which were in the microfloc range, with the largest macrofloc 287 μm in diameter. There is quite clearly a bi-modal clustering of the floc mass; the 80–120 μm fraction contained the prime mode of 35%, with a further 37% of the floc mass distributed throughout the remainder of the microflocs. Compositionally, most of the Central Bay microflocs were less than 30% porous and had

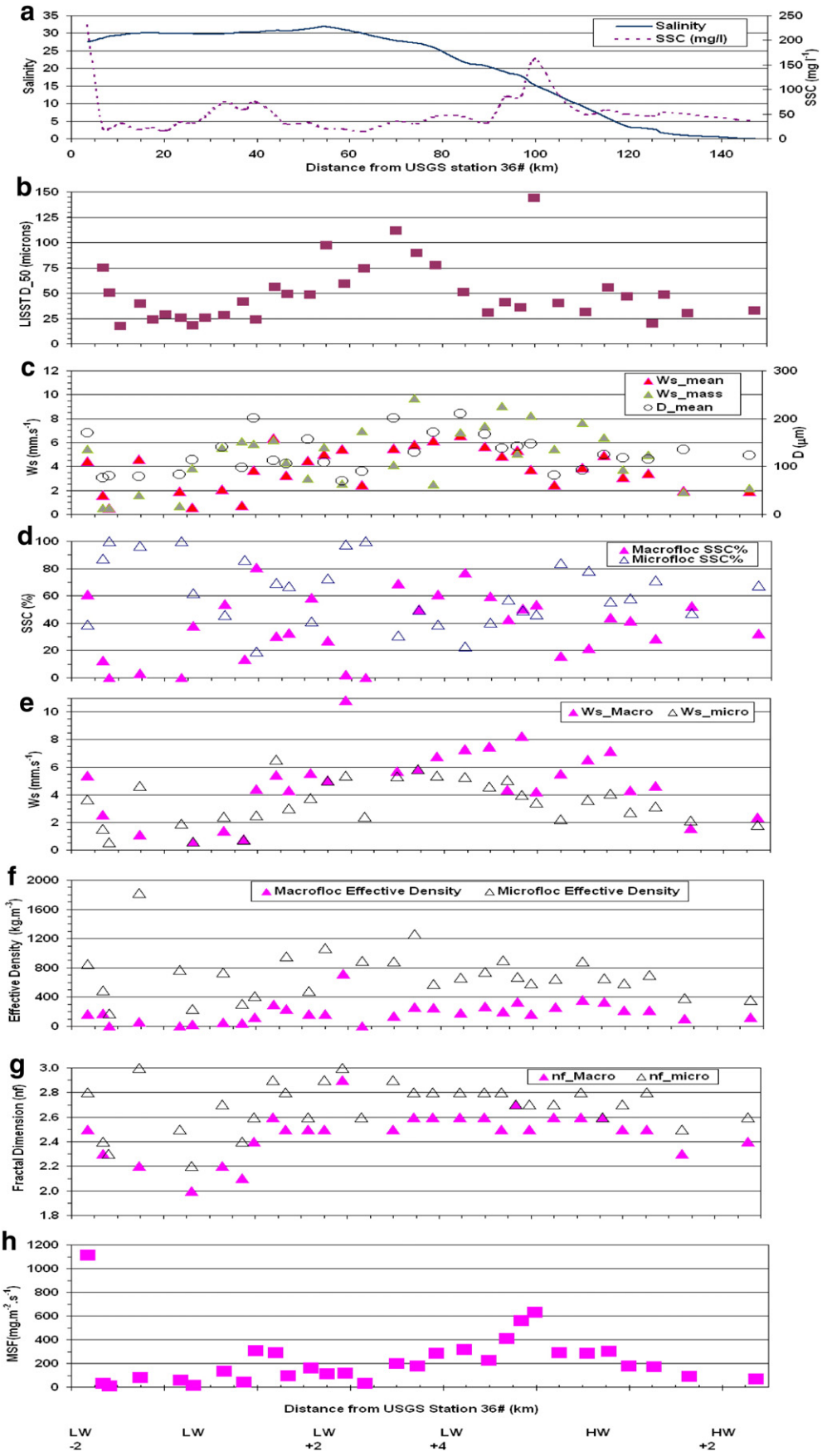

Fig. 4. Time series illustrating the longitudinal variation of the floc properties in SFB: a) salinity and SSC, b) LISST-100 D_{50}, c) Mean floc size, mean and mass-weighted settling velocities, d) Macrofloc & microfloc SSC distributions, e) Macrofloc & microfloc settling velocities, f) Macrofloc & microfloc effective densities, g) Macrofloc & microfloc fractal dimensions and h) MSF. All floc samples were collected at a nominal height of 0.7 m above the estuary bed. The distance from USGS Reference Station 36# and relative tidal state are both indicated on the y-axis.

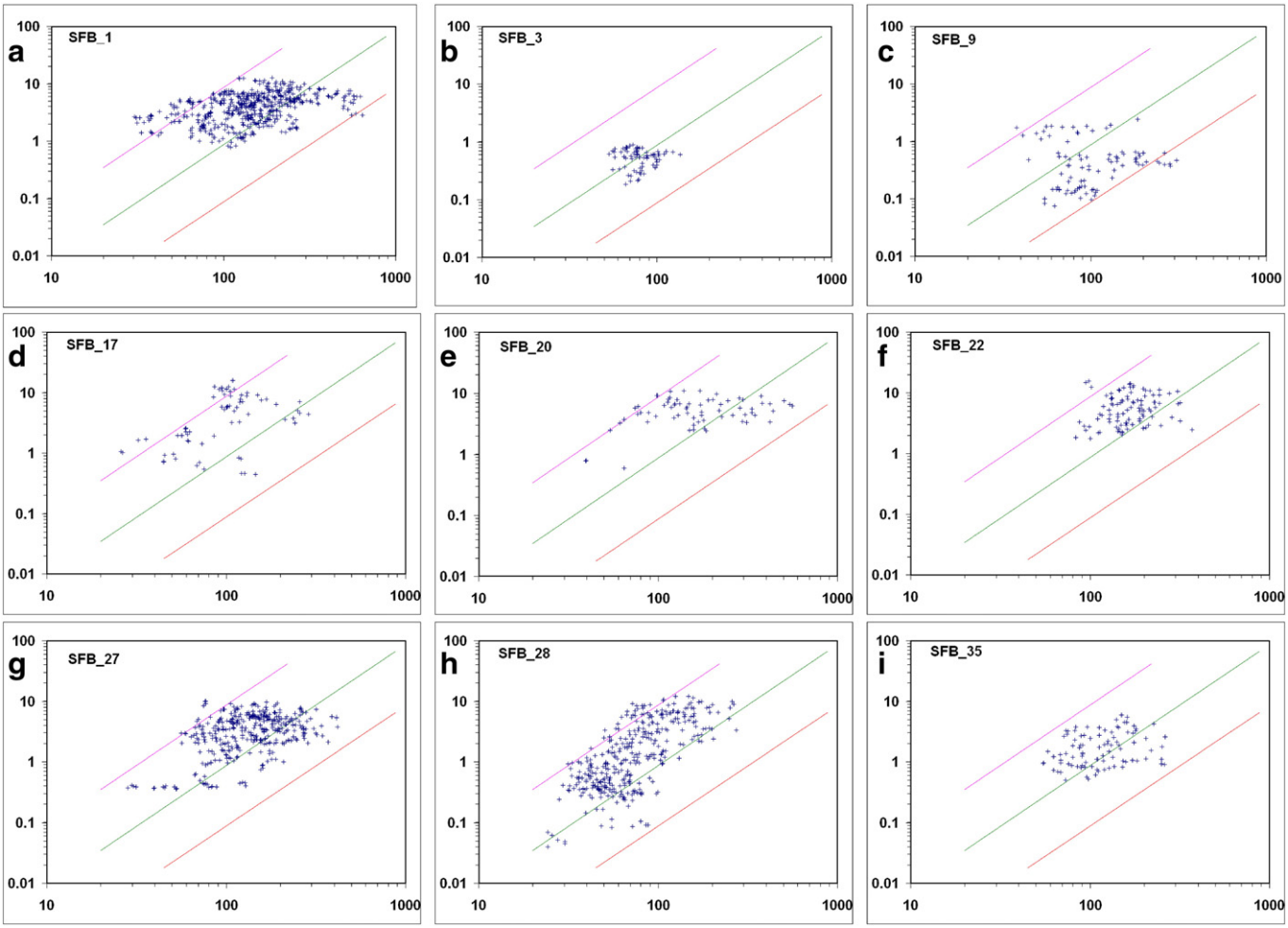

Fig. 5. Nine floc populations with Ws on the y-axes (mm/s) vs. D on the x-axes (microns) for San Francisco Bay floc samples. Diagonal lines on each scatterplot represent contours of constant Stokes equivalent effective density: pink = 1600 kg·m^{-3}, green = 160 kg·m^{-3} and red = 16 kg·m^{-3}. All floc samples were collected at a nominal height of 0.7 m above the estuary bed.

effective densities exceeding 1200 kg·m^{-3}. The microflocs typically exhibited high fractal dimensions of 2.8–3. There are also a number of fine sand particles present. Contrastingly, the macroflocs were more porous (68–91%) and on average were six time less dense (ρ_{e_macro} = 167 kg·m^{-3}) than the average microfloc. The average nf_{macro} was 2.5. Individually, the SFB_17 settling velocities ranged from 0.44 mm·s^{-1} to 15.8 mm·s^{-1}.

In contrast to Central Bay, the TMZ floc population SFB_27 from Carquinez Strait (Fig. 5g) appears more representative of a typical floc population from a predominantly muddy estuarial environment. The largest macroflocs in the TMZ were 419 μm in diameter, which was 132 μm larger than those from Central Bay. However the average fall velocities of both microflocs and macroflocs were 32% and 17% slower than the corresponding floc fractions from Central Bay, respectively. The slower settling rates, coupled with a larger size range, resulted in a shift in the TMZ floc population composition towards more porous, less dense flocs. The SFB_27 microflocs mean effective density was ~592 kg·m^{-3} (porosity ~53%); half the density of the Central Bay microflocs. The TMZ microfloc fractal dimension was 2.7, suggesting that they may be more organically based and contain less sand than those encountered in Central Bay. The TMZ macroflocs ρ_{e_macro} was 164 kg·m^{-3} and the nf_{macro} was 2.5 (porosity ~87%), all of which were similar to Central Bay macroflocs.

The Suisun Bay flocs (SFB_28; Fig. 5h) demonstrated a similar settling velocity range to flocs observed in the TMZ (0.1–10 mm·s^{-1}), but they now exhibited a D_{max} of 273 μm; a size reduction of 146 μm (40%) from the Carquinez Strait TMZ largest flocs. One can see that the majority of the Suisun Bay flocs were clustered between the 160 and 1600 kg·m^{-3} effective density contours, with only a few (25 of 352 observed flocs) small, slow settling (Ws < 0.3 mm·s^{-1}) microflocs (55–100 μm in diameter) possessing ρ_e less than 100 kg·m^{-3}. These low density, small microflocs were 94–98% porous, which suggests they are of a biological origin.

On reaching the freshwater riverine environment of Rio Vista (SFB_35; Fig. 5h), the maximum floc size remained the same as Suisun Bay (SFB_28), but the settling velocities had slowed by 50% to a Ws_{max} of 6 mm·s^{-1}. The SFB_35 flocs were fairly tightly clustered, spanning just over a 200 μm range. Similarly, the settling velocities spanned a much tighter range, with the very slow settling, sub-100 μm fraction observed in SFB_28 no longer present. Instead, there was a significant fraction (32 flocs from the total population of 93) of very low density (ρ_e < 140 kg·m^{-3}) flocs greater than 100 μm at Rio Vista, which exhibited settling velocities spanning the majority of the sample range.

5.3. Hydrodynamic influence

The flocculation process is dependent on both the SSC and turbulence. Throughout the cruise, the majority of the nearbed turbulent shear stresses fell within the 0.2–0.5 Pa range (see Fig. 2 and Table 2), with a complete transect τ_{mean} of 0.33 Pa, which nominally stimulates the ideal inter-particle collision rate to produce the most efficient rate

of floc growth, without creating excessive shearing which can lead to macrofloc breakup, for both purely cohesive (Manning, 2004a) and mixed sediment (Manning et al., 2009) flocs. Therefore we can interpret the majority of the floc data collected throughout the SFB cruise, as being representative of populations favouring their maximum macrofloc growth potential, in a quasi-equilibrium state for the ambient SSC.

Mass-weighted settling velocity varied with the current speed with a hysteresis loop and time lag. The cruise started near the end of ebb tide and water was decelerating (Fig. 6). Settling velocity decreased near slack tide as larger flocs deposited. As the water column initially accelerated at the beginning of flood tide, Ws_{mass} remained less than 2 mm·s^{-1}. Settling velocity increased during the flood tide and this increase lagged the current speed increase. During the maximum flood tide the Ws_{mass} was 2–10 mm·s^{-1}. The optimal linear regression fit between settling velocity and current speed was achieved with a 39 min lag of current speed (Fig. 7). As the lag was increased from 0 to 39 min the correlation coefficient increased slightly from 0.43 to 0.47. The correlation coefficient decreased back to 0.43 for a lag of 60 min and it decreased rapidly as the lag increased greater than 60 min.

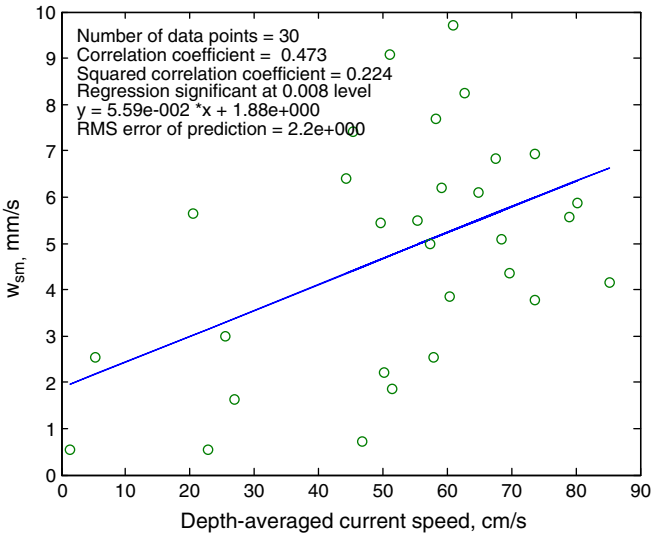

Fig. 7. Correlation between mass-weighted settling velocity Ws_{mass} and depth-averaged current speed lagged by 39 min. All floc samples were collected at a nominal height of 0.7 m above the estuary bed. A 39 min lag produced the best linear correlation.

6. Discussion

6.1. Longitudinal variations

The data (see Figs. 3 and 4) indicates that the longitudinal distribution of settling velocity generally decreased at the end of the cruise landward through Suisun Bay and the lower Sacramento River; locally this is called the low salinity zone. Water depth at the South Bay stations was about 10 m, so any floc with a settling velocity of 2.8 mm·s^{-1} or greater would deposit on the bed during a typical one hour slack tide. Flocs with settling velocities larger than 1–2 mm·s^{-1} are absent near slack tide, so faster settling flocs deposited near slack. The 147 km length of the transect precludes truly synoptic sampling, resulting in sampling during different tidal phases.

Mass-weighted settling velocity was best related to depth-averaged current speed. Greater hydrodynamic energy supports faster-settling flocs in suspension. The response of settling velocity to current speed is delayed by 39 min possibly due to the time needed for resuspension to suspend sufficient sediment to make faster settling flocs and the time needed for flocculation to make faster settling flocs. A floc with a settling velocity of 5 mm·s^{-1} will settle 12 m in 39 min in still water near slack tide. The mean lower low water depth at the sampling stations was 16 m, a similar distance. Thus, the time for fast settling flocs to settle out of the water column appears to be an additional factor contributing to the observed time lag.

Comparisons of our results to previous studies of cohesive sediment in San Francisco Bay sometimes are in agreement and sometimes not. Settling velocity was not fully dependent on SSC (Fig. 8). These results are consistent with Krone (1962), who found that flocs freely settled for SSC less than 300 mg·l^{-1}. Maximum SSC in our study was 230 mg·l^{-1}. Unlike Kranck and Milligan (1992), we did not directly observe an increase in large flocs as SSC increased (Fig. 9). The populations of the two high SSC samples (SFB_1 in South Bay and SFB_27 within the TMZ) both were more than 35% macroflocs. The less turbid (SFB_13) floc population was nearly two thirds macroflocs. The latter stages of Central Bay and through San

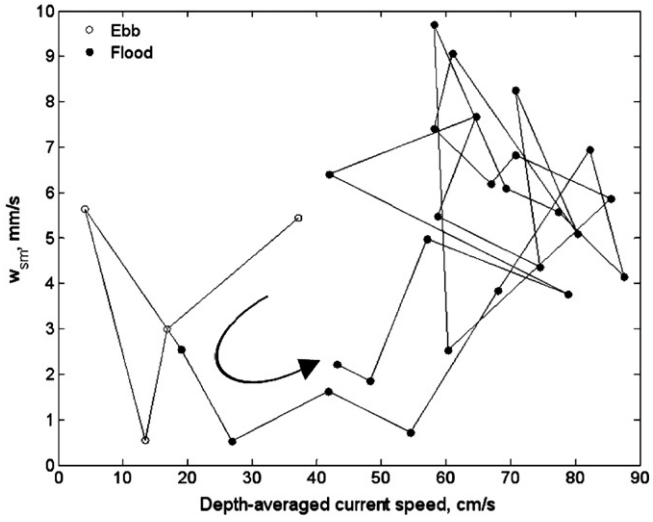

Fig. 6. Mass-weighted settling velocity Ws_{mass} as a function of depth-averaged current speed. All floc samples were collected at a nominal height of 0.7 m above the estuary bed. The curved arrow and lines between data points indicate progression with time. Relative tidal state is also indicated.

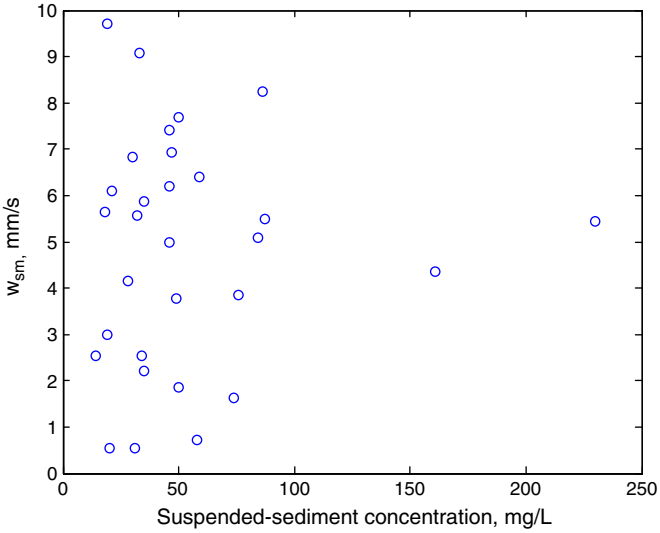

Fig. 8. Mass-weighted settling velocity Ws_{mass} as a function of suspended sediment concentration (SSC). All floc samples were collected at a nominal height of 0.7 m above the estuary bed.

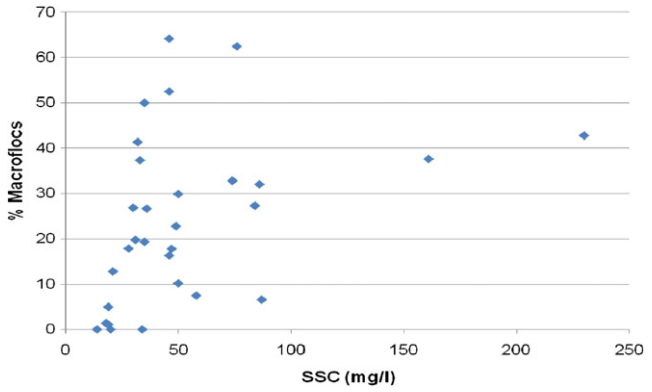

Fig. 9. Macrofloc percentage (by number) for each floc population as a function of suspended-sediment concentration (SSC). All floc samples were collected at a nominal height of 0.7 m above the estuary bed.

Pablo Bay, consistently revealed floc samples which were composed of 30–65% macrofloc.

Our floc diameters were similar to those observed by Kineke and Sternberg (1989, 100–450 μm), but our settling velocities (0.5–10 mm·s^{-1}) were larger (0.5–2 mm·s^{-1}). These latter two studies were at a fixed point in San Pablo Bay over a tidal cycle rather than along a longitudinal transect. They were conducted about 21 years before our study and weeks before an invasive clam became the dominant benthic species in the Bay, which probably increased benthic filtering of the water column (Carlton et al., 1990). This would probably increase bioflocculation, floc density, and settling velocity as observed.

With the exception of the slow settling flocs observed in the latter stages of the cruise in the freshwaters of the Sacramento River, salinity in general, appears to have very little influence on floc size distributions throughout the Bay system as a whole. Krone (1963) found that flocculation quickly reaches an equilibrium situation at a salinity of about 5 for SFB sediment. This agrees with measurements by Burt (1986) in the Thames Estuary (UK), who found no significant correlation between the ambient salt induced electrolyte level and floc size; and the observations of smaller, slower settling flocs within more marine conditions (Eisma and Li, 1993). Therefore, organic content is most probably contributing more towards increasing particle cohesion through raising collision efficiency and hence producing more strongly bonded floc structures.

6.2. Data acquisition issues

The macroflocs and microflocs sub-populations, together with the Ws_{mass}, demonstrated parameterised settling velocities which collectively spanned 0.5 mm·s^{-1} to 11 mm·s^{-1}; this was double the range of the Ws_{mean}. If it was only possible to measure the sample average fall velocity (e.g. from using a device such as a field settling tube), this would produce an under-estimation of the fall velocity distribution.

Spatially, the macroflocs tended to dominate the suspended mass (up to 77% of the ambient SSC) from San Pablo Bay through to Carquinez Strait (the vicinity of the TMZ). Microfloc mass was particularly significant (typically 60–100% of the SSC) in the northern section of South Bay and most of Central Bay. Knowledge of these SSC divisions highlights the importance of knowing the dynamics of the macrofloc and microfloc populations in SFB, and when coupled with the corresponding settling velocities, these parameters are vital for accurate MSF modelling. The video-based INSSEV-LF instrument meets these data acquisition requirements because it measures diameter and settling velocity of individual flocs.

Although video floc sampling devices can produce the various floc property trends observed in SFB, good survey practice is still paramount. One can see that if the sampling coverage (i.e. data collection frequency) is poor, this could lead to potential mis-interpretations of the data and only limited conclusions may be drawn from such a restricted survey. For example: The average of the macrofloc settling velocities observed for all 30 stations of the SFB transect was a Ws_{macro} of 4.8 mm·s^{-1}. Now if floc sampling was only conducted at only every fourth stations along the transect (e.g. due to limited boat time, and cost restrictions), the transect mean Ws_{macro} slows by nearly 40% to 2.9 mm·s^{-1}. Similarly, the limited transect gives the impression that the macroflocs only represent 23% of the ambient SSC. When in reality, the more comprehensive 30 station transect indicates that over 37% of the suspended matter were present as macroflocs.

In terms of locations throughout SFB, the limited survey (i.e. only 3 stations) suggests that the average Ws_{macro} for South Bay slows to 1.5 mm·s^{-1} and the respective SSC_{macro} was 9.7%. Whereas the full survey (10 stations in South Bay) reveals that the limited survey has under-estimated both the macrofloc SSC distribution by a massive factor of four and the fall rate by a factor of two. In the marine environment of Central Bay, a limited survey (a single observation at Point Blunt; SFB_17) again showed a four-fold under-estimate in the macrofloc suspended mass (full survey $SSC_{macro} = 38\%$) and a 25% lower settling velocity (full survey $Ws_{macro} = 6.3$ mm·s^{-1}).

At the less saline region of SFB, when attempting to capture a synoptic snap-shot of the TMZ flocs, sampling at numerous consecutive locations through the Carquinez Strait (i.e. SFB_25 to 28), produces an average Ws_{macro} of 6.2 mm·s^{-1} and shows the macroflocs comprising 53% of the ambient SSC. In contrast, a single point observation at Crockett (SFB_25) reveals a macrofloc settling velocity which was nearly 2 mm·s^{-1} slower and 10% less macrofloc mass. Therefore, one can see how poor coverage of SFB, can result in very misleading interpretations of both the Bay as a whole and selected regions of SFB.

Typically fixed station Eulerian measurements are often the choice for numerical model calibration. However, these data tests have shown that the level of flocculation which determines the floc diameter, density, and settling velocity, all vary significantly longitudinally in estuary. The floc growth implies large variations in the sediment settling flux with direct implications on the vertical distribution of sediment loading. This suggests that in order to gain an accurate spatial insight into the floc dynamics throughout a system the size of SFB (145 km transect), collecting samples from 30 sites provides an average coverage resolution of one sample every 4.8 km and can provide a much better picture of floc dynamics throughout SFB. 25–30 measurements appear to provide sufficient redundancy in order to obtain representative floc parameters. Ideally a combination of a small number of fixed (Eulerian) stations coupled with La Grangian monitoring, is the only way to provide adequate coverage of the sediment transport dynamics in a large system for numerical model calibration. This is analogous to the use of a single beam echo sounder coupled with a side-scan sonar, in order to produce high quality bathymetry data: the greater the distance between the survey lines, the more reliance which is placed on the side-scan sonar data to spot anomalies and maintain a high level of accuracy/consistency between survey points. Therefore good quality spatial data of floc population properties are required in order to predict sediment pathways.

6.3. Mixed sand and mud flocs

Previous research has shown that estuaries which are regarded as predominantly muddy, tend to produce floc populations which exhibit slow settling microflocs coupled with a significantly faster settling macrofloc fraction (e.g. Gibbs, 1985; van Leussen, 1994; Manning, 2004a, 2004b). Furthermore, for purely muddy estuaries, the macroflocs are usually more abundant and dominate the floc dry mass.

For many of the SFB samples (e.g. SFB_9, 12, 14, 17, 20 and 21), both the Ws_{macro} and Ws_{micro} are very closely matched (10% apart). Also the major portion of the floc mass is in the form of microflocs

for half of the samples (see Fig. 4). This all strongly suggests that the flocs are not composed solely of pure muddy sediments. Suspended sediment in San Francisco Bay is predominantly fine sediment with a small amount of sand. The median mass fraction of sand-sized material (greater than 63 μm) in 35 Bay water samples collected from November 2005 to January 2006 collected from several sites was 98%, the mean was 96.4%, standard deviation 5.8%, minimum 66.5%, maximum 99.8%. In many instances where the re-entrained mud and sand operate in an entirely independent fashion, this is referred to as a segregated suspension (van Ledden, 2002). If the sediments were segregated, there would be a clear demarcation in terms of the particle density, with solid, non-flocculated mineral grains clustering on or beyond the 1600 $kg \cdot m^{-3}$ effective density contours on Fig. 5. However there is a clear floc density transition present, with many microflocs demonstrating ρ_e of 600–1200 $kg \cdot m^{-3}$. This is indicative of mixed sediment flocculation, whereby mud and sand co-exist as a single mixture (Mitchener et al., 1996) and this creates the potential for these two fractions to combine and exhibit some degree of interactive flocculation (Manning et al., 2009).

The existence of cohesion developing in sediment mixtures has been identified by a number of researchers including Dyer (1986) and Raudkivi (1998), who demonstrated that a clay content of just 5–10% can cause natural sediment mixtures to behave in a cohesive manner. Assisted by the mediation of sticky organic polymers, such as EPSs (Tolhurst et al., 2002), sand grains can potentially become encapsulated within a muddy 'cage-like' structure (Whitehouse et al., 2000). With the solid sand grains forming part of the floc matrix, the high porosity and volume of interstitial water normally associated with pure mud flocs have been dramatically reduced. This results in a mixed sediment floc having a density which is less than a pure quartz grain, but significantly more dense than typical mud flocs. The source of the EPS could be the result of phytoplankton blooms within the Bay; such high levels of biological activity are known to encourage flocculation (Kranck and Milligan, 1988) and this eventually increases the cohesiveness of the deposited sediments.

These mixed sediment flocs are clearly present throughout the SFB, but especially within Central Bay. For example, closer examination of sample SFB_17 (Fig. 5h) which is potentially a mud:sand mixture, reveals that the Ws_{micro} was 5 $mm \cdot s^{-1}$, which was only 0.1 $mm \cdot s^{-1}$ slower than the Ws_{macro}. The SFB_17 microflocs also accounted for three quarters of the 21 $mg.l^{-1}$ SSC. In comparison, the muddier suspension located within the TMZ (sample SFB_27) showed that although the 236 microflocs out-numbered the larger macroflocs by nearly a ratio of 2:1, both fractions contributed fairly equally to the floc mass (see Fig. 4d).

In terms of the MSF, the more abundant microfloc mass present in SFB_17 accounted for 86 $mg \cdot m^{-2}\ s^{-1}$ (75%) of the 115 $mg \cdot m^{-2}\ s^{-1}$ total flux. Over half of the mixed sediment MSF originated from the 80–120 μm sized microflocs. The dominance of the microflocs within flocculating mud:sand mixtures has been reported by Whitehouse and Manning (2007) for Tamar Estuary mud mixed with fine sand. Whilst in the more cohesive TMZ, the SFB_27 macroflocs and microflocs contributed more equally to the total MSF of 633 $mg \cdot m^{-2}\ s^{-1}$. The latter is similar to floc distributions observed in purely cohesive suspensions within the Tamar Estuary and Gironde Estuary during neap tides (see Manning, 2004a,b).

If we compare the relative settling flux dynamics of SFB_17 and SFB_27, we see that the quicker fall rates of both the microfloc and macrofloc from the Central Bay sample result in a MSF of 5.5 $mg \cdot m^{-2}\ s^{-1}$ per $mg \cdot l^{-1}$ of SSC. This compares to just 3.9 $mg \cdot m^{-2}\ s^{-1}$ per $mg \cdot l^{-1}$ of SSC within the TMZ sample. It must be noted that the settling flux is only an indication of the potential for deposition. The net settling flux is only part of the total vertical particle flux which consists of the settling flux and the turbulent entrainment flux. Depending on which one dominates, one has either deposition or entrainment.

6.4. Fractal dimension

Fractals are often used to mimic flocculation, but a number of authors have found that single average fractal dimensions do not always correctly represent the characteristics depicted by natural flocs (e.g. Dyer and Manning, 1999; Mehta et al., 2009). The data reveals that sample mean fractal dimensions ranged from 2.2 to 3 throughout the transect. Correspondingly, the average nf_{macro} for the entire transect was 2.4, nearly 0.25 less than the denser microfloc fraction. The nf_{macro} was only 2 midway through South Bay (SFB_9) and rose to 2.9 in Central Bay (SFB_18). The nf_{micro} were 2.2 and 3 for the same locations, respectively.

If we examine the fractal dimension variations through South Bay sample SFB_9, we see that individual floc nf values at the lower end of the scale were nf of 1.8, which corresponds to both the largest macrofloc (D = 308 μm with a Ws of 0.47 $mm \cdot s^{-1}$) and 54 μm diameter microfloc, which had a settling velocity of just 0.08 $mm \cdot s^{-1}$; an order of magnitude difference for both D and Ws values. At the other end of the scale, only a 40 μm microfloc with a Ws of 1.4 $mm \cdot s^{-1}$ produced a nf value of 3. This demonstrates the wide range in fractal dimensions within just a single floc population.

Ganju et al. (2007) applied fractal theory to LISST size data in order to estimate Ws in areas throughout San Francisco Bay. Ganju et al. (2007) hypothesised that the floc diameter and density relation was fairly constant in San Francisco Bay because the primary particles and flocculation mechanisms were spatially homogeneous. With the exception of SFB_1, the fairly consistent settling velocities values (Ws_{mass} of 0.6–1.5 $mm \cdot s^{-1}$) observed during the ebb in the lower portion of South Bay seem to partly confirm this hypothesis. However for the remainder of the transect, Ws_{mass} ranged from 2 to 9.7 $mm \cdot s^{-1}$. If we examine the work of Ganju et al. (2007), their conclusions were based on instruments that measure populations of particle size (i.e. using a LISST and SSC to obtain volume concentration, then relating particle density = mass concentration divided by volume concentration) and the effect of the population on light (turbidity), not on direct measurements of individual particles (i.e. as with the INSSEV_LF). We hypothesise that the different interpretations are due to the ability to quantify individual particles (as with INSSEV_LF) rather than solely populations of particles.

Furthermore, Ganju et al. (2007) found that fractals did not correctly represent SFB flocs in the near-bed region, which resulted in their estimated settling velocities being too low. This could potentially be due to a number of reasons. Muddy sediment is composed of both clay minerals and organic matter, but fractal theory requires a single primary particle size to be assigned, which is difficult to determine. This issue is magnified with mixed flocculating sediments, as the fine sand is also added to the floc matrix, thus reducing further the potential for geometric self-similarity.

Additionally, we also need to consider the operation of the LISST-100 instrument and how realistic the sizes measured by this laser diffraction device based on Mie scattering theory are within a mild to moderately turbid estuary (Agrawal et al., 2008). If we look at the D_{50} LISST data collected during the June 17th 2008 survey, within the potentially mixed sediment environment of South and Central Bay, some LISST sizes match fairly well with the INSSEV-LF D_{mean}, whilst other samples show the LISST reporting a three or four-fold undersizing. In addition, combining fractal theory and size-only observations, poorly estimate settling velocity because variations in floc density are neglected.

7. Conclusions

Floc sizes measured at 30 stations, nominally 0.7 m above the estuary bed in San Francisco Bay, ranged from 24 μm to 639 μm, whilst settling velocities ranged between 0.04 $mm \cdot s^{-1}$ and 15.8 $mm \cdot s^{-1}$ during the longitudinal transect. Mass-weighted mean settling velocities

(Ws_{mass}) generally ranged from 0.5 $mm \cdot s^{-1}$ to 10 $mm \cdot s^{-1}$. 3D hydrodynamic modelling data indicated that the majority of the nearbed turbulent shear stresses throughout the transect duration were within the 0.2–0.5 Pa range which nominally stimulates the ideal inter-particle collision rate to produce the most efficient rate of floc growth, without creating excessive macrofloc breakup (Manning, 2004a). The macrofloc and microfloc sub-populations demonstrated parameterised settling velocities which spanned double the range of the Ws_{mean}. The macroflocs tended to dominate the suspended mass (up to 77% of the ambient SSC) from San Pablo Bay through to Carquinez Strait (the vicinity of the TMZ). Microfloc mass was particularly significant (typically 60–100% of the SSC) in the northern section of South Bay and most of Central Bay.

Slack tide in South Bay allowed larger and faster settling flocs to deposit which accounts for most of the longitudinal variability. The best single predictor of settling velocity was the current flow velocity 39 min prior to sampling, not suspended-sediment concentration or salinity. Resuspension and settling lags are likely responsible for the lagged response of settling velocity to water velocity. The distribution of individual floc diameters and settling velocities indicates that floc density for a given floc diameter varies greatly. A small portion (a few percent) of suspended sediment mass in SFB is sand-sized and inclusion of sand in flocs appears likely.

Fractal theory for cohesive sediment assumes that there is a single primary particle size that flocculates, which is not the case for these mixed sediment flocs. The wide variability in the physical, biological and chemical processes which contribute to flocculation within SFB, mean that spatial floc data is required in order to accurately represent the diverse floc dynamics present in the Bay system. Similarly, no single settling velocity will adequately mimic the MSF distributions throughout SFB.

The importance in determining accurate estimates of floc effective density has been highlighted by the SFB data, as these provide the basis for realistic distributions of floc dry mass and the mass settling flux across a floc population. Significant errors in floc density calculation can arise through incomplete data sets (e.g. just floc size observations without settling velocity data, or vice versa), or unjustified theoretical assumptions (e.g. employing a fractal geometric relationship to floc data, when it is evident that the flocs are not composed from a single base primary particle size). This study has demonstrated that these density errors can be significantly reduced by simultaneously measuring floc size and settling velocity across the full range of flocs which constitute an entire population, on a repeatable basis. The video-based INSSEV-LF instrument meets these data acquisition requirements because it measures diameter and settling velocity of individual flocs. Although this may appear slightly restrictive due to the wide range of floc sampling techniques available, some of which are easier to use and deploy than video devices, the natural variability in the SFB floc characteristics measured during this study demonstrate the importance of acquiring complete floc spectral distribution data of the floc sizes, settling rates and respective floc mass. This is vital if the floc data is to be parameterised and used to calibrate settling fluxes in a numerical sediment transport model of the SFB system.

However, although video floc sampling devices can produce the various floc property trends observed in SFB, good survey practice is still paramount. One can see that if the sampling coverage (i.e. data collection frequency) is poor, this could lead to potential mis-interpretations of the data and only limited conclusions may be drawn from such a restricted survey. For example, a limited survey (i.e. only 3 stations, compared to the 10 stations in the full survey) in South Bay produces an under-estimate in both the macrofloc SSC_{macro} distribution by a factor of four and the Ws_{macro} by a factor of two.

To develop sediment transport numerical models, high quality floc size and settling data are needed to understand and simulate the depositional qualities of both suspended cohesive sediment and mixed sediments in San Francisco Bay. However this study has shown that it is extremely important to parameterise the data correctly. If for instance just a single diameter or settling velocity were used, the decrease in settling velocity at slack tide could not be simulated. One technique to mimic decreased settling velocity at slack tide is to make settling velocity a function of SSC, because SSC decreases, however our data shows that no single function of Ws (SSC) applies to the entire estuary. Another approach would be to use a single mass-weighted settling velocity that is a function of lagged water velocity; this is a significant improvement over Ws_{mean}, but still not ideal for accurate cohesive sediment transport modelling which needs to represent a wide variety of floc populations (see Dyer et al., 1996). Thus, the most pragmatic solution is a physically-based approach, whereby the detailed floc D vs. Ws spectra are parameterised in terms of their macrofloc and microfloc properties. This aids in the model calibration, whilst retaining more of the dynamical aspects of the floc populations (e.g. Lee et al., 2011; Soulsby et al., 2013). All forms of flocculation are dynamically active processes, therefore it is important to also include both SSC and turbulence functions with the floc data.

Acknowledgements

The authors would like to thank Jessica Wood, Scott Wright and the RV Polaris crew (Byron Richards, Scott Conard, Sarah Foster, Cate Phillips, Tara Schraga) for their help and assistance during the San Francisco Bay cruise. We thank Michael MacWilliams of Delta Modeling Associates Inc. for providing hydrodynamic model output. Prof. Manning would like to thank his HR Wallingford Coasts & Estuaries colleagues Prof. Richard Whitehouse and Tim Chesher, for their continued support throughout the SFB surveys. The preparation of this paper was partly funded by both the US Geological Survey Co-operative Agreement Award (G11AC20352) with HR Wallingford (DDS0280) and the HR Wallingford Company Research 'Sediment in Transitional Environments — SiTE' project (DDY0427).

References

Agrawal, Y.C., Pottsmith, H.C., 1994. Laser diffraction particle sizing in STRESS. "Continental Shelf Research 14 (10/11), 1101–1121.
Agrawal, Y.C., Whitmire, A., Mikkelsen, O.A., Pottsmith, H.C., 2008. Light scattering by random shaped particles and consequences on measuring suspended sediments by laser diffraction. "Journal of Geophysical Research 113 C04023.
Alldredge, A.L., Silver, M.W., 1988. Characteristics, dynamics and significance of marine snow. "Progress in Oceanography 20, 41–82.
Benson, T., Manning, A.J., 2013. DigiFloc: the development of semi-automatic software to determine the size and settling velocity of flocs. HR Wallingford Report DDY0427-RT001 (in press).
Burban, P.-Y., Lick, W., Lick, J., 1989. The flocculation of fine-grained sediments in estuarine waters. "Journal of Geophysical Research 94 (C6), 8323–8330.
Burt, T.N., 1986. Field settling velocities in estuarine muds. Coastal and Estuarine Studies, 14. Springer-Verlag, Berlin, pp. 126–150.
Carlton, J.M., Thompson, J.K., Schemel, L.E., Nichols, F.H., 1990. Remarkable invasion of San Francisco Bay (California, USA) by Asian clam *Potamocorbula amurensis*. Introduction and dispersal. "Marine Ecology Progress Series 66, 81–94.
Chassagne, C., Mietta, F., Winterwerp, J.C., 2009. Electrokinetic study on kaolinite suspensions. "Journal of Colloid and Interface Science 336 (1), 352–359.
Cheng, R.T., Casulli, V., Gartner, J.W., 1993. Tidal, residual, intertidal mudflat (TRIM) model and its applications to San Francisco Bay, California. "Estuarine, Coastal and Shelf Science 36, 235–280.
Conomos, T.J., Peterson, D.H., 1977. Suspended-particle transport and circulation in San Francisco Bay, an overview. Estuarine Processes, vol. 2. Academic Press, New York, pp. 82–97.
Delo, E.A., 1988. Estuarine muds manual. Hydraulics Research, Wallingford, Report No. SR164, pp. 23–26.
Droppo, I.G., 2001. Rethinking what constitutes suspended sediments. "Hydrological Processes 15, 1551–1564.
Droppo, I.G., Walling, D., Ongley, E., 2000. The influence of floc size, density and porosity on sediment and contaminant transport. "Journal of the National Centre for Scientific Research 4, 141–147.
Dyer, K.R., 1986. Coastal and Estuarine Sediment Dynamics. Wiley & Sons, Chichester (342 pp.).
Dyer, K.R., Manning, A.J., 1999. Observation of the size, settling velocity and effective density of flocs and their fractal dimensions. "Journal of Sea Research 41, 87–95.

Dyer, K.R., Cornelisse, J.M., Dearnaley, M., Jago, C., Kappenburg, J., McCave, I.N., Pejrup, M., Puls, W., van Leussen, W., Wolfstein, K., 1996. A comparison of in-situ techniques for estuarine floc settling velocity measurements. "Journal of Sea Research 36, 15–29.
Edzwald, J.K., O'Melia, C.R., 1975. Clay distributions in recent estuarine sediments. "Clays and Clay Minerals 23, 39–44.
Einstein, H.A., 1941. The viscosity of highly concentrated underflows and its influence on mixing. "Transactions, American Geophysical Union 597–603 (Hydrology).
Einstein, H.A., Krone, R.B., 1962. Experiments to determine modes of cohesive sediment transport in salt water. "Journal of Geophysical Research 67 (4), 1451–1461.
Eisma, D., 1986. Flocculation and de-flocculation of suspended matter in estuaries. "Netherlands Journal of Sea Research 20 (2/3), 183–199.
Eisma, D., Li, A., 1993. Changes in suspended matter floc size during the tidal cycle in the Dollard Estuary. "Journal of Sea Research 31, 107–117.
Eisma, D., Dyer, K.R., van Leussen, W., 1997. The in-situ determination of the settling velocities of suspended fine-grained sediment — a review. In: Burt, N., Parker, R., Watts, J. (Eds.), Cohesive Sediments — Proc. of INTERCOH Conf. (Wallingford, England). John Wiley & Son, Chichester, pp. 17–44.
Fennessy, M.J., Dyer, K.R., Huntley, D.A., Bale, A.J., 1997. Estimation of settling flux spectra in estuaries using INSSEV. In: Burt, N., Parker, R., Watts, J. (Eds.), Cohesive Sediments — Proceedings of INTERCOH Conference (Wallingford, England). John Wiley & Son, Chichester, UK, pp. 87–104.
Fettweis, M., Francken, F., Pison, V., Van den Eynde, D., 2006. Suspended particulate matter dynamics and aggregate sizes in a high turbidity area. "Marine Geology 235, 63–74.
Ganju, N.K., Schoellhamer, D.H., Murrell, M.C., Gartner, J.W., Wright, S.A., 2007. Constancy of the relation between floc size and density in San Francisco Bay. In: Maa, J.P.-Y., Sanford, L.P., Schoellhamer, D.H. (Eds.), Estuarine and Coastal Fine Sediments Dynamics. Elsevier Science B.V., pp. 75–91.
Garcia, M.H. (Ed.), 2007. Sedimentation Engineering. Garcia, M.H. (Ed.), 2007. American Society of Civil Engineers Manuals and Reports on Engineering Practice, No. 110.
Gibbs, R.J., 1985. Estuarine flocs: their size settling velocity and density. "Journal of Geophysical Research 90 (C2), 3249–3251.
Gilbert, G.K., 1917. Hydraulic-mining Debris in the Sierra Nevada. U.S. Geological Survey Professional Paper 105.U.S. Geological Survey, Government Printing Office, Washington, D.C., USA (154 pp.).
Kimmerer, W.J., Gross, E.S., MacWilliams, M.L., 2009. Is the response of estuarine nekton to freshwater flow in the San Francisco estuary explained by variation in habitat volume? "Estuaries and Coasts 32, 375–389.
Kineke, G.C., Sternberg, R.W., 1989. The effect of particle settling velocity on computed suspended sediment concentration profiles. "Marine Geology 90, 159–174.
Kolmogorov, A.N., 1941a. The local structure of turbulence in incompressible viscous fluid for very large Reynolds numbers. Comptes Sendus de l'Académie des Sciences de l'URSS, 30 (301 pp.).
Kolmogorov, A.N., 1941b. Dissipation of energy in locally isotropic turbulence. "Comptes Rendus de l'Académie des Sciences de l'URSS 32 (16 pp.).
Kranck, K., 1984. The role of flocculation in the filtering of particulate matter in estuaries. In: Kennedy, V. (Ed.), The Estuary as a Filter. Academic Press, Orlando Inc., pp. 159–175.
Kranck, K., Milligan, T.G., 1988. Macroflocs from diatoms: in-situ photography of particles in Bedford Basin, Nova Scotia. "Marine Ecology Progress Series 4, 183–189.
Kranck, K., Milligan, T.G., 1992. Characteristics of suspended particles at an 11-hour anchor station in San Francisco Bay, California. "Journal of Geophysical Research 97 (C7), 11373–11382.
Krone, R.B., 1962. Flume Studies of the Transport of Sediment in Estuarial Shoaling Process: Final Report. Hydraulic Engineering Laboratory and Sanitary Engineering Research Laboratory, University of California, Berkeley, California (110 pp.).
Krone, R.B., 1963. A study of rheological properties of estuarial sediments. Report No. 63–68. Hyd. Eng. Lab. and Sanitary Eng. Lab., University of California, Berkeley.
Krone, R.B., 1986. The significance of aggregate properties to transport processes. In: Mehta, A.J. (Ed.), Estuarine Cohesive Sediment Dynamics. Springer-Verlag, Berlin, pp. 66–84.
Lee, B.J., Toorman, E., Molz, F., Wang, J., 2011. A two-class population balance equation yielding bimodal flocculation of marine or estuarine sediments. "Water Research 45, 2131–2145.
MacWilliams, M.L., Salcedo, F.G., Gross, E.S., 2008. San Francisco Bay–Delta UnTRIM model calibration report. POD 3-D Particle Tracking Modeling Study, Prepared for California Department of Water Resources, 19th December 2008 (344 pp. See: http://science.calwater.ca.gov/pdf/workshops/POD/2008_final/GrossMacWilliams_POD_UnTRIM_Calibration_Report.pdf).
Manning, A.J., 2001. A Study of the Effects of Turbulence on the Properties of Flocculated Mud. Ph.D. Thesis Institute of Marine Studies, University of Plymouth, Plymouth, UK (282 pp.).
Manning, A.J., 2004a. The observed effects of turbulence on estuarine flocculation. "Journal of Coastal Research 41, 90–104 (Special Issue, SI).
Manning, A.J., 2004b. Observations of the properties of flocculated cohesive sediment in three western European estuaries. "Journal of Coastal Research 41, 70–81 (Special Issue SI).
Manning, A.J., 2006. LabSFLOC — A Laboratory System to Determine the Spectral Characteristics of Flocculating Cohesive Sediments. HR Wallingford Technical Report, TR 156.
Manning, A.J., Dyer, K.R., 2002. The use of optics for the in-situ determination of flocculated mud characteristics. "Journal of Optics A: Pure and Applied Optics 4, S71–S81.
Manning, A.J., Baugh, J.V., Spearman, J., Whitehouse, R.J.S., 2009. Flocculation settling characteristics of mud:sand mixtures. "Ocean Dynamics. http://dx.doi.org/10.1007/s10236-009-0251-0.
Manning, A.J., Schoellhamer, D.H., Mehta, A.J., Nover, D., Schladow, S.G., 2010. Video measurements of flocculated sediment in lakes and estuaries in the USA. Proceedings of the Joint Federal Interagency Conference on Sedimentation and Hydrologic Modeling, Riviera Hotel, Las Vegas, Nevada, USA, 27th June–1st July 2010.
Manning, A.J., Spearman, J.R., Whitehouse, R.J.S., Pidduck, E.L., Baugh, J.V., Spencer, K.L., 2013. Laboratory assessments of the flocculation dynamics of mixed mud: sand suspensions. In: Manning, A.J. (Ed.), Sediment Transport Processes and their Modelling Applications. Intech, Rijeka, Croatia. ISBN: 978-953-51-1039-2, pp. 119–164. http://dx.doi.org/10.5772/3401.
McAnally, W.H., Mehta, A.J., 2001. Collisional aggregation of fine estuarine sediments. In: McAnally, W.H., Mehta, A.J. (Eds.), Coastal and Estuarine Fine Sediment Processes — Proc. in Mar. Sci., 3. Elsevier, Amsterdam, pp. 19–39.
McCave, I.N., 1984. Size spectra and aggregation of suspended particles in the deep ocean. "Deep-Sea Research 31, 329–352.
McKee, L.J., Ganju, N.K., Schoellhamer, D.H., 2006. Estimates of suspended sediment flux entering San Francisco Bay from the Sacramento and San Joaquin Delta, San Francisco Bay, California. "Journal of Hydrology 323, 335–352.
Mehta, A.J., 1989. On estuarine cohesive sediment suspension behaviour. "Journal of Geophysical Research 94 (C10), 14303–14314.
Mehta, A.J., Jaeger, J.M., Valle-Levinson, A., Hayter, E.J., Wolanski, E. and Manning, A.J., 2009. Resuspension dynamics in Lake Apopka, Florida. Final Synopsis Report, submitted to St. Johns River Water Management District, Palatka, Florida, June 2009, Report No. UFL/COEL-2009/00, 158p.
Mie, G., 1908. Beiträge zur Optik trüber Medien, speziell kolloidaler Metallösungen. Leipzig. "Annalen der Physik 330, 377–445.
Mikeš, D., Manning, A.J., 2010. An assessment of flocculation kinetics of cohesive sediments from the Seine and Gironde Estuaries, France, through laboratory and field studies. "Journal of Waterway, Port, Coastal, and Ocean Engineering (ASCE) 136 (6), 306–318. http://dx.doi.org/10.1061/(ASCE)WW.1943-5460.0000053.
Mitchener, H.J., Torfs, H., Whitehouse, R.J.S., 1996. Erosion of mud/sand mixtures. "Coastal Engineering 29, 1–25 (Errata, 1997, 30, 319).
Oseen, C.W., 1927. Neuere methoden und ergebnisse. Hydrodynamik. Akad Verlagsges, Leipzig.
Overbeek, J.T.G., 1952. Kinetics of flocculation. Colloid Science, volume 1, chapter VIII, H.R. Kruyt (ed), L.C. Jackson (translator), Elsevier, Amsterdam, p. 278–300.
Owen, M.W., 1976. Determination of the settling velocities of cohesive muds. Hydraulics Research, Wallingford, Report No. IT 161 (8 pp.).
Partheniades, E., 1962. A Study of Erosion and Deposition of Cohesive Soils in Salt Water. PhD Thesis University of California, Berkeley (June 1962).
Pouët, M.-F., 1997. La Clarification Coagulation — Flocculation. Traitement de l'eau potable cours. EMA, option Environnement et Systèmes Industriels.
Raudkivi, A.J., 1998. Loose Boundary Hydraulics, 3rd edition. Balkeme, Rotterdam.
Ruhl, C.A., Schoellhamer, D.H., 2004. Spatial and temporal variability of suspended-sediment concentrations in a shallow estuarine environment. "San Francisco Estuary and Watershed Science 2 (2) (article 1)/http://repositories.cdlib.org/jmie/sfews/vol2/iss2/art1S.
Schoellhamer, D.H., 2001. Influence of salinity, bottom topography, and tides on locations of estuarine turbidity maxima in northern San Francisco Bay. In: McAnally, W.H., Mehta, A.J. (Eds.), Coastal and Estuarine Fine Sediment Processes — Proc. in Marine Science, 3. Elsevier, Amsterdam. ISBN: 0-444-50463-X, pp. 343–357.
Schoellhamer, D.H., Lionberger, M.A., Jaffe, B.E., Ganju, N.K., Wright, S.A., Shellenbarger, G.G., 2005. Bay Sediment Budgets: Sediment Accounting 101: The Pulse of the Estuary: Monitoring and Managing Water Quality in the San Francisco Estuary. San Francisco Estuary Institute, Oakland, California 58–63 (See: URL http://www.sfei.org/rmp/pulse/2005/RMP05_PulseoftheEstuary.pdf).
Schoellhamer, D.H., Mumley, T.E., Leatherbarrow, J.E., 2007. Suspended sediment and sediment-associated contaminants in San Francisco Bay. "Environmental Research 105, 119–131.
Soulsby, R.L., Manning, A.J., Spearman, J., Whitehouse, R.J.S., 2013. Settling velocity and mass settling flux of flocculated estuarine sediments. "Marine Geology. http://dx.doi.org/10.1016/j.margeo.2013.04.006.
Stratton, A., 1941. Electromagnetic Theory. McGraw-Hill, New York.
Tolhurst, T.J., Gust, G., Paterson, D.M., 2002. The influence on an extra-cellular polymeric substance (EPS) on cohesive sediment stability. In: Winterwerp, J.C., Kranenburg, C. (Eds.), Fine Sediment Dynamics in the Marine Environment — Proceedings in Marine Science, 5. Elsevier, Amsterdam, pp. 409–425.
van Ledden, M., 2002. A process-based sand–mud model. In: Winterwerp, J.C., Kranenburg, C. (Eds.), Fine Sediment Dynamics in the Marine Environment — Proc. in Mar. Science, 5. Elsevier, Amsterdam. ISBN: 0-444-51136-9, pp. 577–594.
van Leussen, W., 1994. Estuarine Macroflocs: Their Role in Fine-grained Sediment Transport. PhD thesis University of Utrecht (488 pp.).
van Leussen, W., 1997. The Kolmogorov microscale as a limiting value for the floc sizes of suspended fine-grained sediments in estuaries. In: Burt, N., Parker, R., Watts, J. (Eds.), Cohesive Sediments. Wiley, New York, pp. 45–73.
Whitehouse, R.J.S., Manning, A.J., 2007. Mixing It: How Marine Mud and Sand Interact, 71. Innovation & Research Focus, Institution of Civil Engineering, London, Thomas Telford Services Ltd., p. 2.
Whitehouse, R.J.S., Soulsby, R., Roberts, W., Mitchener, H.J., 2000. Dynamics of Estuarine Muds. Thomas Telford Publications, London (232 pp.).
Winterwerp, J.C., 1998. A simple model for turbulence induced flocculation of cohesive sediment. "Journal of Hydraulic Research 36 (3), 309–326.
Winterwerp, J.C., van Kesteren, W.G.M., 2004. Introduction to the physics of cohesive sediment in the marine environment. In: van Loon, T. (Ed.), Developments in Sedimentology, 56. Elsevier, Amsterdam (466 pp.).
Wright, S.A., Schoellhamer, D.H., 2005. Estimating sediment budgets at the interface between rivers and estuaries with application to the Sacramento–San Joaquin River Delta, Water Resources. "Research 41. http://dx.doi.org/10.1029/2004WR003753 W09428.
Xu, R., 2000. Particle Characterization: Light Scattering Methods. Kluwer Academic Publishers, Dordrecht.